Most important changes in the manuscript:

1. **Update of literature list with new and younger references (most of them in the introduction section).**
2. **Detailed statements on the focus of this study incl. a list of objectives in the introduction section.**
3. **Deletion of Section 2.3 and the corresponding equations.**
4. **Implementation of new Section 4.5 on the discussion of future field applications in the given context.**

Response to the Editor

Two referees thoroughly evaluated the manuscript, and the authors answered in detail to the comments. Most of these comments have been addressed appropriately. Still, I would like to emphasize some important issues the authors still should focus on when revising the manuscript. Beside all given comments by the reviewers these include particular the following points:

All reformulations and new passages announced with the reply letters to the reviewers were realised except of those concerning the Editor's points no. 1 and 2 (see explanations below).

1) possible challenges with field application should be put into the discussion and not the conclusion chapter

1) The discussion on this issue is now given in the new section 4.5. With this additional section the concerns of RC1 regarding field applicability and the concerns of RC2 regarding the potential of T2 measurements are considered.

2) I agree to keep the rather long theory because it is helpful for readers not very familiar with the topic; still try to shorten parts if possible as it indeed is very lengthy

2) The original section 2.3 and the corresponding equations have been deleted after reformulating the most important statements from it into section 2.2. This includes a short discussion on existing empirical approaches for estimating permeability that was recommended by RC2.

3) it should be at least mentioned in the manuscript that synthesis procedures for the iron oxides have been verified earlier

3) Done: at the end of the corresponding passage describing the procedure of the iron oxide synthesis in section 3.1.

4) thoroughly check for recent, important references to strengthen your introduction.

Done: additional references were included as announced with the replies to the reviewers

Response to Reviewer 1:

General Comments

The paper addresses an interesting and important topic and does help to advance geophysics in the field of hydrogeology. It demonstrates that the NMR method is applicable to characterize zones with iron oxides accumulations, being used in well characterization and hydraulics. The manuscript is well written, but especially ant the methods section to lengthy. It would be better to shorten it. The results are well presented. In the conclusion, I would recommend to stronger emphasize the difficulties one would expect to use NMR in the field, in contrast to the lab study presented.
Thank you for the positive feedback. Regarding the shortening we do not fully agree, please see our response below (response to P3 ff, chapter 2.2 and 2.3). However, Section 2.3 from the old manuscript has now completely been deleted, while the most important statements are reformulated into Section 2.2. The discussion on expected possible difficulties in the field according to the reviewer's recommendation is now given in a new Section 4.5 (along with a similar recommendation of RC2)

Specific comments and technical details

The introduction does not capture the current state of the art; most of the literature is outdated and new papers missing.
We do not fully agree with this general assessment. Regarding the literature with focus on the building processes for iron-oxides we have added some newer references. Regarding the NMR-related literature we think that the given references are state of the art with publishing dates up to 2017. However, we do not agree with the general idea that important findings can be "outdated" – only because the corresponding research was made decades ago. Given that these "older" research results are still relevant for our current work, we prefer to consider the corresponding publications directly and to appreciate in this way the work of the corresponding involved research pioneers. Thus most of the older references are still included.

In the methods section the textbook knowledge should be deleted.
We do not agree to avoid references to textbooks. They are an important source for comprehensive background information for the interested reader.

XRD data need to be added in the revision in order to proof mineralogy.

The synthesis procedures for ferrihydrite and goethite as applied in this study have been verified many times for decades (e.g. Cornell and Giovanoli, 1987; Janney et al., 2000), so we do not think that it is necessary to provide that proof another time. Moreover, the contents of Fe-minerals in our samples are far below 2 wt-%, so quantitative (and even qualitative) detection of the precipitates via XRD would be at least difficult, if not even impossible. We added a statement on the reliability of the used recipes and provide references that successfully applied them in the past (Section 3.1).

P2, L1: do not repeat "vital". Please make clear more specific what is "vital" to you, avoid generalizing.
Agreed, in addition to the repetition of the word "vital" in these two sentences, they exhibit some redundancy, anyway. According to the reviewer's recommendation, we have reformulated the passage including new literature.

You may want to include the role of iron in nutrient cycling and biology. Please also do not cite several times a textbook like Schwertmann and Cornell. Cite recent research literature.
We've added additional references on that topic, please see the response on P2L1 above.

P2, L6: avoid self-citation if not necessary. There is nice literature from others. So far, the literature used is not sate of the art. New and important literature is missing completely in the introduction so far. Include this carefully in the revision.

We've added additional references also at this place in addition to Houben et al. (2003). However, we do not agree to avoid self-citation, if the corresponding references is precise. This is the case here, so we'd like to keep Houben (2003) in.

P2, L13: Sorry, your literature is outdated. I will not comment this further. You need to include the current state of the art. Please invest carefully time to update your paper
We've added additional references of younger age here and at other places. However, as already mentioned above: in our opinion there is no outdated literature, if the corresponding findings are still relevant and to-the-point. Proper acknowledgement to the pioneers of important research is just fair. Therefore, we'd like to keep most of the older papers in.

P3, L15: please make the goals of this paper after the setting you used clear to the reader
Agreed. RC2 gave a similar recommendation in her general comments. We've added a passage at the end of the introduction section clarifying our goals.

P3 ff, chapter 2.2 and 2.3: please shorten this drastically. This is a research paper and not a student textbook or master thesis. Do not re-state things that can be read elsewhere. If you use formulae in the following, do so if needed for the paper.
We have deleted Section 2.3, while reformulating the most important statements from it into Section 2.2. Regarding Section 2.2, we do not agree with the reviewer's assessment. It is true, the mathematics in this section is a reproduction of given knowledge. However, it is not (yet) standard knowledge in geoscience! The basis of this theory was already manifested by Brownstein and Tarr (1979) in the seventies, but their focus was the application of NMR relaxometry in biological cells. Established textbooks on NMR with geophysical background treat the appearance of slow diffusion regimes as exotic behavior with negligible relevance for geomaterials, which might be true for sandstones, claystones, shales, and carbonates – potential host rocks for hydrocarbon resources. (Please remember that geophysical NMR applications were developed for oil exploration in the first place.)

Regarding the growing field of NMR research for aquifer and soil characterisation, we are convinced that pore spaces in the slow diffusion regime are much more relevant, which is proven by many recent experimental research activities (Grunewald and Knight, 2011; Keating and Knight, 2012; Müller-Petke et al., 2015). However, we lack of approaches to treat such behaviour when interpreting NMR relaxation data of soils and sediments. Our study is an important step towards bridging this gap and we feel that it is still necessary to summarise and emphasise the underlying theory.

In addition, the whole bunch of equations in chapter 2.2 is needed to understand and reproduce the data-fitting scheme that we apply and reproducibility is a necessity for scientific papers in the first place.

P7 and 8: you need to add XRD data to show you actually produced ferrihydride and not a mixture of other iron oxyhydroxides
XRD data was not acquired, because the iron contents were too low for a proper analysis. Please see our comments above.

Response to Reviewer 2:

General comments:
This is an interesting paper and addresses the importance of iron oxides on NMR signals, in this case focusing on T1 relaxation. And authors also probed into the relationship between surface relaxitivity $\rho 1$ and iron content. The structure and organization of this manuscript is good, and the presentation of the data is also satisfactory. The authors covered a lot of topical areas: impact of paramagnetic materials, novel NMR relaxation analysis, and so on. I feel a bit lost about the focus and the main findings of this paper. There are couple of other issues and suggestions
Thank you for the positive feedback. Regarding the main objectives of this study, we've added a clarifying passage in the introduction section (See also the comment of RC1 on P3L15).

1. Pore size distribution estimation from particle size distribution is not reliable. The NMR mode analysis is based on the assumption of narrow (single) pore, I feel it is difficult to be convinced for this particular experiments as iron oxide precipitation would generate much smaller pores. This is a crucial point as the authors use reff information intensively, including calculating the diffusion regime. The updated reff could significantly alter the results and interpretation. Additionally, surface area analysis (i.e., BET) could help authors answer few ambiguous observations, e.g., the difference in surface relaxitivity between goethite and ferrihydrite.

We agree that estimates of pore size distribution (PSD) from grain size distribution (GSD) are of less plausibility. However, in soil physics it is common practice to use pedotransfer functions to estimate cumulative pore size distributions (=water retention functions) from texture information (e.g. Cornelis et al., 2001; Schaab et al., 2001). Consequently, the general judgement "not reliable" does not hold. Although not relevant for the paper, we want to refer to these publications:

- *Cornelis, W.M., Ronsys, J., van Meirvenne, M., Hartmann, R. (2001): Evaluation of pedotransfer functions for predicting the soil moisture retention curve. Soil Sci. Soc. Am. J. 65, 638-648.* ***=> 227 citations***
- *Schaap, M.G., Leij, F.J., van Genuchten, M.Th. (2001): Rosetta: a computer program for estimating soil hydraulic parameters with hierarchical pedotransfer functions. J. Hydrol. 251, 163-176.* ***=> 1459 citations***

Moreover, we do not estimate pore size distributions but a single effective pore size in this study. Estimating effective hydraulic quantities from grain size distributions is a very reliable and proven concept. Consequently, many geologists have used those approaches for decades. Beginning with pure empirics by Hazen (1892) and followed by many others continuously fine-tuning the basic idea (see e.g. Vukovic and Soro, 1992; Boadu 2000; Chapuis and Aubertin, 2003; Glover and Walker, 2009; and the references therein), the reliability of estimating hydraulically effective measures from grain size distributions has been proven many times. Besides the traditional empirical approach of Hazen (1892), we decided to apply in addition a modern approach with physical background: the approach of Carrier (2003) who includes also the content of the smallest particles in the grain size distribution yielding a more reliable estimate of the effective radius. We think another proof that the principle idea works is beyond the scope of this paper. We just make use of a proven concept to test our results.

- *Boadu (2000): Hydraulic Conductivity of Soils from Grain-Size Distributions: New Models. Journal of Geotechnical and Geoenvironmental Engeneering 126 (8).*
- *Chapuis, Robert & Aubertin, Michel. (2003). Predicting the coefficient of permeability of soils using the Kozeny-Carman equation. Département des génies civil, géologique et des mines, Ecole Polytechnique de Montréal, Montreal, 2003.*
- *P. W. Glover and E. Walker (2009): Grain-size to effective pore-size transformation derived from electrokinetic theory GEOPHYSICS, 74(1), E17-E29. doi.org/10.1190/1.3033217.*
- *Vuković, Milan & Soro, Andjelko (1992). Determination of hydraulic conductivity of porous media from grain-size composition. Water Resources Publications, Littleton, Colo*

We also agree that iron oxide precipitation can lead to small particles. These particles and possibly their intrinsic porosity can be hydraulically relevant if they accumulate and clog the pore throats between the quartz grains. As explained in the Material section, our sample preparation was made with the focus on coating and an iron oxide distribution inside the sample holders as homogeneous as possible. Consequently, the iron oxide coats the surface of the very most samples, whereas additional small particles hardly occur. To support this statement, we've added the grain size distribution curves as supplement to depict visually the minor amount of iron oxide particles against the predominating quartz grains (please see Fig.S1). As already described along with Fig.7a in the manuscript, only for the samples with iron oxide content > 1 g/kg, the effective hydraulic cross-section, i.e. the effective pore radius, starts to decrease. Even for these three samples, as for the others, the volume fraction of the pore space between few iron oxide particles can be assumed to be negligible. Please remember that our iron contents do not exceed 0.6 % by weight. So, we are convinced that our assumption of narrow pore size distributions holds for all investigated samples.

We also agree that the BET method is very capable to analyse the surface of iron oxide minerals (see e.g. Houben and Kaufhold, 2011) and it was actually our idea as well to measure it along with this study. However, the surface area of the samples was smaller than the accuracy limit of the device and, unfortunately, the results are of no use for us to quantify the difference between the ferrihydrite and goethite coatings in this case. A note was added in the Section 3.1 with comments on our BET measurements.

2. Can the authors discuss on the choice of coarse grain size particles? Also discuss what if the particles are fine.

For small pores the fast diffusion regimes holds, for which a calibration is necessary to quantify pore-size related information. This case is treated in many publications and corresponding references are already given in the manuscript. Our choice on coarse sand and gravel was due to the fact that there are many open questions on the estimation of hydraulic properties for these materials.

We've added a passage in the introduction section to clarify the focus on coarse material in this study. The principle difference between large and fine pores regarding NMR relaxation theory is discussed in section 2.2.

3. In the study, only T1 relaxation has been studied (T2 was only used to calculate porosity). T2 relaxation is more important and it would be necessary to conduct T2 experiments and analysis. If both T1 and T2 measurements are obtained, more parameters like $\rho 1/\rho 2$ can be extracted to provide insights of NMR monitoring of iron oxides. Why the authors didn't consider using low-field NMR core analyzer instead of one-side NMRMouse?

Agreed, T2 is important as it is certainly the method of choice in borehole practice. However, this is a scientific study on the principle relation of NMR relaxation and pore size. Using T1 measurements for the analysis we can ensure to exclude systematic bias by internal or external gradient fields in B0. These must always be considered when working with T2. Even if using a core analyser with perfect homogeneous B0 (perfect homogeneity is actually not possible), internal gradient fields might occur, especially if working with iron inside the investigated material. It is important at this state to quantify the pore surface related NMR effects first. The analysis of T2 with its specific problems and limitations is the second step, which will be part of our future research. We already had a discussion in the manuscript on the future role of T2 in practical application. However, this passage is now copy-and-pasted into an extra Section 4.5 (Discussion chapter) and extended in consideration of RC2's comment No 3 along with a similar recommendation of RC1 in his/her general comments:

A serious problem of the experiments in this study was the heterogeneity of the samples, as already explained in the manuscript at P7L30ff and depicted in Fig. 5 and in the supplement. Using the NMR Mouse instead of a core analyser, we could be sure to control and verify homogeneity of the iron oxide distribution. Using a core scanner, the entire sample is measured at once. We expected misinterpretation due to overlay of different relaxation regimes inside the sample caused by varying

content of iron oxide particles over the sample. The reasoning for using the NMR Mouse instead of a common Core Analyser is stressed now with additional sentences at the beginning of section 3.4.

4. Similar to the first comment, the hydraulic conductivity should be measured in the lab to compare with NMR estimated value (from equation 12).

Direct measurements of hydraulic conductivity should certainly be preferred if possible. However, in this case those measurement would not have been reasonable:

a. The material had to be repacked, which leads to different porosity, packing density and hydraulic conductivity. We assessed those measurement to be of limited value compared to the estimation from the GSD.
b. We worried about material wash out in the corresponding flow experiments immediately after NMR, which would have disabled the entire reference analysis. This analysis (XRF, grain size, BET), on the other hand, was assessed to be more essential than flow experiments.
c. The portion that could have been reserved for flow experiments after subdividing the samples for the reference analysis was much too small to be a significant representative of the sample for determining hydraulic conductivity. In addition, experimental problems are expected regarding the small sample size in combination with coarse material. Due to high hydraulic conductivities and short flow distances, pressure loss in the material is very low and barely measureable. For reliable calculation of hydraulic conductivity, longer flow distances, i.e. larger sample sizes are essential. However, larger samples were not an option due to the requirements for the chemical treatment.

Finally, we have chosen the effective radius approach as our reference method here. Our future experiments will combine NMR and flow experiments. A note on that outlook is now given in the Conclusions.

Specific comments:

1. Intro – The significance of studying iron oxide in saturated porous media is beyond the control of negative incrustations. I suggest authors consider making a broader argument of the importance of such study.

Agreed, we've added a passage in the introduction to emphasise the importance also for soils and aquifers. See also the response on the comment of RC1 on P2L1.

2. Intro – line 16 to 17 on page 2. The introduction of applying geophysical methods seems too sudden. The aim of this study would be better to placed after the introduction of NMR relaxometry. I think the effect of iron oxide (or paramagnetic materials in general) on NMR (surface relaxitivity) needs to further reviewed, and more references should be added here.

Agreed with both points:

1. The passage has been reformulated to introduce the demand of geophysical methods in the given context.
2. The history of systematic studies on paramagnetic effects on NMR has been added.

3. Basics of NMR – line 16-17 on page 5, I didn't follow how to simplify ξn to $(n + 1/2)2\pi 2$. Can authors further explain (use formula if applicable)/

The quantitative meaning of this equation is not relevant for us, only its quality: the fact that the relaxation in the slow diffusion regime is independent from the surface relaxivity. As described and discussed in (new) section 2.3 (=old section 2.4) along with Fig.1 and in section 4.3 along with Fig.7b, we found proof that this pure analytical/mathematical statement holds in practice. Following the suggestion of RC1 not to overload the paper with mathematics that can be found elsewhere, we refer to the original paper (Brownstein and Tarr, 1979) for the mathematical details in this particular case.

4. Basics of NMR 2.4 – Do the authors assume single dominate pore size in analyzing the data? Can authors elucidate the applicability of Müller-Petke et al., (2015)'s conclusion in this study? For example, what characteristics of the samples used in this study to make this single pore size assumption valid?

Detailed information on the samples would be misplaced here in the theory section, i.e. before the material is introduced in the section material and methods. However, RC2 is right, the reasoning for the approach of Müller-Petke et al. (2015) appears too late in the old version of the manuscript. Thus, we give now an additional statement at the beginning of section 2.3 (=old section 2.4) to motivate the approach of Müller-Petke et al. (2015).

In addition, we've added a more detailed reasoning at the beginning of section 3.6.

5. Basics of NMR 2.4 – Did you do similar intensity and ρr/D simulation and parameter search for T2 relaxation? Does the same conclusion hold?

Regarding the theory of NMR relaxation in porous media, no differences in the T_2,surf (Eq.4) term are expected. Regarding the data quality, on the other hand, one could expect advantages if using T2 for a similar approach because smaller relaxation times are better represented in the T2 data. These signals appear with higher amplitudes against the noise. However, reliable T2 simulation must consider T_2,Diff (Eq.4), which must be identified individually for a given device (=influence of external B0 gradient) and a given material (= influence of internal B0 gradient). This analysis and interpretation is far beyond the scope of this paper, but must be considered in future work on T2 in the given context. Corresponding notes on the outlook on future T2-NMR applications have been added in the discussion section (new Section 4.5).

6. Page 6, repeated use of the word 'unambiguous', consider changing some of it to other words like 'nonunique'.

The word is used twice in section 2.3 (=old section 2.4) with more than 20 lines between the two. We do not feel the necessity to change the wording.

7. Basics of NMR 2.4 – Could the authors define what are apparent surface relaxitivity and apparent pore radius? Equivalent value or NMR estimated value? The last sentence of this section 'An important objective of this study is the comparison …' seems to be a bit lost in the context. If this is an important objective, I suggest the authors review the relationship between rapp NMR and reff.

Agreed, we have reformulated the corresponding sentence introducing these quantities to clarify that these are NMR-estimated parameters.

8. Material and methods – I suggest the authors use a flowchart to facilitate the explanation of the sample preparation and iron coating treatment. Why the authors didn't measure the reff using MICP or imaging analysis? The estimation of reff from particle size is not reliable. If the authors want to compare the reff with rapp NMR, a realistic estimation of reff from analytical characterization is necessary.

We agree that imaging analysis can yield r_eff estimates as well, given that a representative region of the sample is captured, i.e. enough pores are observed to verify the result by statistics. However, there is a conflict regarding the resolution especially if working with coarse material. To satisfy the requirement above, the investigated specimen must be large enough, which comes at the price of lowering the resolution. We expect that it is very difficult to balance resolution and representative sample size for the material in this study and we are sure to get into a serious discussion about the resolution problem, which would be beyond the scope of this paper. This study is focused on the effective quantities NMR can provide in the given context and as explained above we are convinced that the effective radii estimated from the GSD are qualified as reference data.

However, we accept the suggestion of RC2 and will include quantitative imaging analysis into our future research facing the challenge of finding a reliable trade-off between resolution and statistics. A note on imaging analysis has been added in the Conclusions as outlook for future research.

9. Material and methods – line 18 page 8. ‘due to the high proportion of quartz, contents of siliceous iron are generally expected to be very low in fresh filter sand’. Does it mean the siliceous iron content is extremely low due to high purity of SiO2?

Yes, the most filter sands are usually very pure quartz. However, this sentence is irrelevant and has been deleted. Instead, we give now an additional note on the actual quantification of the amount of siliceous iron in our samples in section 3.1. Material and methods – 3.4 why B0 has a strong gradient in *z* direction? Inhomogeneities in permanent magnets? Could you elaborate on this? I’m curious to know.

The magnetic field strength naturally decreases with increasing distance to the magnet, therefore the gradient cannot be avoided for the NMR-Mouse. For details please see the original paper(s). The corresponding sentence has been extended to clarify this fact.

10. Results and discussion – 4.1 page 11 line 22 and line 30‘the latter exhibits a relaxation time of less than 0.2 s’, it didn’t seems to be 0.2s to me from the figure. Why coarse material will contribute to uncertainties in porosity estimation?

Reply on P11L22: The relaxation time marks the point on the T2 curve, where the initial signal amplitude E0 is decreased down to E0/e=E0/2.7183, which corresponds to 1.4715 for the data of the pure water in Fig. 4a. At this point, the time axis counts 0.2 s. No changes necessary.

Reply on P11L30: It is an issue of the reference volume (see e.g. Costanza-Robinson et al., 2011): with decreasing sample dimension (L in the figure below), the porosity estimate (n in the figure below) gets more and more inaccurate. The sentence at P11L30 has been reformulated in the manuscript to underline this effect for our experiments more clearly.

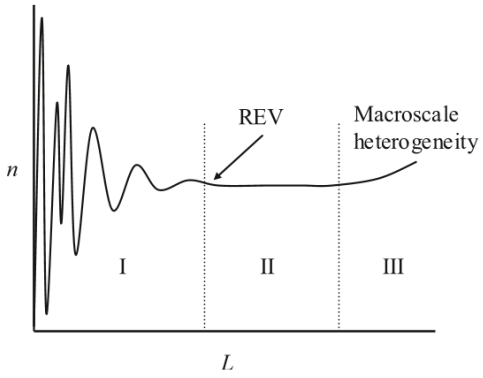

Source: *Costanza-Robinson et al. (2011). (For details see the updated reference list of the revised manuscript)*

11. Results and discussion – 4.2 What is the scanning interval in your experiments? I thought you use 8 measurements at different depths for each sample, but the data points on figure 5 look much more than 8.

The reviewer is right. We used a scanning increment of 1 mm for all NMR measurements, which leads to more than eight measurements for the sample holders before homogenisation, which are larger than the sample holders after homogenisation. This is clarified now in Section 3.4.

12. Results and discussion – 4.2 ‘This assumption is acceptable because the grain size distribution and consequently also the pore size distribution is narrow for the well-sorted materials studied here’ This statement is not convincing. I would expected a quite broad range (at least bimodal) of pore size distribution as much smaller iron oxide precipitation occurred. Especially authors also pointed out that rapp gets smaller when iron content increased. As I brought up before, the estimation of pore size distribution from grain size distribution is not convincing and the authors need to show evidence of pore size distribution from analytical measurements.

As explained above (see response on the general comments No.1), we …

a. do not share the opinion of RC2 regarding the estimation of hydraulically effective measures from the GSD
b. consider the pore space between the iron particles to be of less importance regarding their content of less than 1% by weight.

Thus, we hold to our interpretation scheme of using r_eff and the corresponding hydraulic conductivity estimates from GSD as reference values to verify the NMR results.

13. Results and discussion – 4.2 Did the authors calculate K using other models like SDR or Coates model? How did it compare to the K estimation using equation 12? Which equations you used to calculate KKC and 2.20 KHz? Did you actually measure K in the lab for different samples? It is very necessary to do such measurements.First,

The reviewer is focusing on empirical standard models (SDR – Schlumberger-Doll-Research and Coates, 1999) that are normally used for interpreting NMR well logging data. However, these models do not apply here.

First, they work only in the fast diffusion regime, where a linear relationship of relaxation times and pore size is given and every pore is represented by a unique relaxation time. These conditions are excluded for the samples in this study.

Second, these models need a calibration on the surface relaxivity which is expected to change in every sample due to the individual amount of paramagnetic surface coating. That means, the application of these models demands an individual hydraulic-conductivity calibration for each sample, which makes the estimation of the hydraulic conductivity pointless.

To mention that these approaches exist and to clarify that they do apply only under fast diffusion conditions, we added additional notes in Section 2.2.

Hydraulic characterisation of iron oxide-coated sand and gravel based on nuclear magnetic resonance relaxation modes analyses

Stephan Costabel[1], Christoph Weidner[2, 3], Mike Müller-Petke[4], Georg Houben[2]

[1]Federal Institute for Geosciences and Natural Resources, Berlin, Wilhelmstraße 25 - 30, 13593, Germany
[2]Federal Institute for Geosciences and Natural Resources, Hannover, Stilleweg 2, 30655, Germany
[3]Current address: [3]North Rhine Westphalian State Agency for Nature, Environment and Consumer Protection, Recklinghausen, Leibnizstr. 10, 45659, Germany
[4]Leibniz Institute for Applied Geophysics, Hannover, Stilleweg 2, 30655, Germany

Correspondence to: Stephan Costabel (stephan.costabel@bgr.de)

Abstract. The capability of nuclear magnetic resonance (NMR) relaxometry to characterise hydraulic properties of iron oxide-coated sand and gravel was evaluated in a laboratory study. Past studies have shown that the presence of paramagnetic iron oxides and large pores as present in coarse sand and gravel disturbs the otherwise linear relationship between relaxation time and pore size. Consequently, the commonly applied empirical approaches fail when deriving hydraulic quantities from NMR parameters. Recent research demonstrates that higher relaxation modes must be taken into account to relate the size of a large pore to its NMR relaxation behaviour in the presence of significant paramagnetic impurities at its pore wall. We performed NMR relaxation experiments with water-saturated natural and reworked sands and gravels, coated with natural and synthetic ferric oxides (goethite, ferrihydrite) and show that the impact of the higher relaxation modes increases significantly with increasing iron content. Since the investigated materials exhibit narrow pore size distributions, and can thus be described by a virtual bundle of capillaries with identical apparent pore radius, recently presented inversion approaches allow for estimating a unique solution yielding the apparent capillary radius from the NMR data. We found the NMR-based apparent radii to correspond well to the effective hydraulic radii estimated from the grain size distributions of the samples for the entire range of observed iron contents. Consequently, they can be used to estimate the hydraulic conductivity using the well-known Kozeny-Carman equation without any calibration that is otherwise necessary when predicting hydraulic conductivities from NMR data. Our future research will focus on the development of relaxation time models that allow for broader pore size distributions. Furthermore, we plan to establish a measurement system based on borehole NMR for localising iron clogging and controlling its remediation in the gravel pack of groundwater wells.

1 Introduction

Iron oxides are, due to their abundance and reactive properties, amongst the most important mineral phases in the geosphere (Cornell and Schwertmann, 2003; Colombo et al, 2014). They encompass a variety of oxides, hydroxides and oxihydroxides of predominantly ferric iron but all are referred to as iron oxides in this study for the sake of brevity. They form some of the most important commercial iron ores worldwide but also play a vital role in soils and aquifers. As weathering products, iron oxides control the conditions for soil genesis and degradation (Stumm and Sulzberger, 1991; Kappler and Straub, 2005) and the mobility of nutrients, trace metals, and contaminants (Cornell and Schwertmann, 2003; Colombo et al., 2014; Cundy et al., 2014). Particularly in many tropic and subtropic soils, the building processes of iron-oxide exhibit high temporal dynamics and may change the environmental conditions within a few years, which makes it necessary to further develop measurement techniques to characterise and monitor the corresponding status of soils and aquifers.~~They form some of the most important commercial iron ores worldwide but also play a vital role in soils and aquifers, where they control the mobility of trace metals and nutrients (Cornell and Schwertmann, 2003). As weathering products, iron oxides play a vital role in many tropic and subtropic soils and aquifers, where their appearance controls the infiltration/evaporation conditions, vegetation, soil degradation, and groundwater recharge processes.~~

Furthermore, iron oxides play a negative role when forming in wells and drains used for the extraction of fluids from the subsurface, e.g. in drinking water production, oil wells, dewatering of mines or bogs, landfill leachate collection systems and geothermal energy systems (Houben, 2003a; Larroque and Franceschi, 2011; Medina et al., 2013). The formation of iron oxide incrustations negatively affects the performance of these systems by blocking the entrance openings and the pore space of gravel pack and formation (Weidner et al., 2012). The removal of such deposits is expensive and time-consuming. Their spatial distribution is often inhomogeneous (Houben and Weihe, 2010; Weidner, 2016). It is therefore imperative to identify their exact location and to characterise their degree of clogging to successfully target rehabilitation measures. Ideally, this is to be done before the incrustation gained a state at which fluid movement through the pore space is significantly hindered in order to ensure maximum chance of success of the remediation activities. Although the chemical (~~McBain, 1901; Haber and Weiss, 1934;~~ Stumm and Lee, 1960~~, 1961; Davison and Seed, 1983~~; Pham and Waite, 2008; Geroni and Sapsford, 2011; Larese-Casanova et al., 2012) and biological processes (~~Ehrlich et al., 1991;~~ Tuhela et al., 1997; Cullimore, 2000; ~~Weber et al., 2006~~Emerson et al., 2010) involved are well investigated, accurate methods for identifying and characterising the location and degree of iron-mineralisation in situ are still not available.

Geophysical field and borehole methods have the potential to comply with this demand. Methods such as electrical resistivity tomography, electromagnetics, and ground penetrating radar are sensitive to different phases and concentrations of iron oxides in the pore space (e.g. van Dam et al., 2002; Atekwana and Slater, 2009; Abdel Aal et al., 2009). The same is true for the method of nuclear magnetic resonance (NMR, e.g. Bryar et al., 2000; Keating and Knight, 2007, 2008, 2010). The aim of this laboratory study is to assess the potential of NMR for identifying ~~When applying geophysical investigation methods (e.g. electrical resistivity tomography, electromagnetics, ground penetrating radar), different phases and concentrations of iron oxides in the pore space can affect the result and must be taken into account accordingly (e.g. van Dam et al., 2002; Atekwana and Slater, 2009; Abdel Aal et al., 2009). The aim of this laboratory study is to assess the potential of nuclear magnetic resonance (NMR) methods for identifying~~ the location and concentration of iron oxide coatings in water-saturated porous media and the assessment of their hydraulic effects.

Geophysical applications of NMR relaxometry are used in hydrocarbon exploration, hydrogeology, environmental and soil sciences for estimating pore liquid contents, pore size distributions, and permeability ~~(e.g. Kenyon, 1997; Hinedi et al., 1997; Blümich et al., 2008)~~. When applied in boreholes and laboratory, NMR is able to identify different pore fluid components, e.g. water and oil (e.g. Bryar and Knight, 2003; Hertzog et al., 2007), to distinguish between clay-bound, capillary-bound and mobile pore water (e.g. Prammer et al., 1996; ~~Behroozmand et al., 2014~~Coates et al., 1999; Dunn et al., 2002), and to provide hydraulic and soil physical parameters (e.g. Dlugosch et al., 2013; Costabel and Yaramanci, 2011, 2013; Sucre et al., 2011; Knight et al., 2016). As non-invasive tool from the subsurface, it is used for investigating the subsurface distributions of water content/porosity and hydraulic conductivity and allows for the lithological categorisation of aquifer and aquitards (e.g. Legchenko et. al., 2004; ~~Mohnke and Yaramanci, 2008;~~ Costabel et al., 2017).

NMR relaxometry for hydraulic characterisation of porous media takes advantage of the paramagnetic properties of the pore surface. The NMR measurement observes the exchange of energy between stimulated proton spins of the pore fluid and the

pore walls and thereby provides a proxy for pore surface-to-volume ratios, i.e. pore sizes. However, existing approaches to estimate pore sizes and permeabilities demand material-specific calibration (Kenyon 1997, Coates et al., 1999), which is expected to be particularly difficult for materials containing a large amount of paramagnetic species (Keating and Knight, 2007). Moreover, NMR relaxation measurements are affected by additional effects such as the occurrence of additional energy losses within the pore fluid (Bryar et al., 2000; Bryar and Knight, 2002), ferromagnetism and corresponding disturbances of the magnetic fields (Keating and Knight, 2007, 2008), and the existence of pore geometries with a high level of complexity, e.g. capillaries with angular cross sections or fractal pore surfaces (Sapoval et al., 1996; Mohnke et al., 2015; Müller-Petke et al., 2015). Different iron oxide phases can produce any of these effects and can thus significantly bias the results. Foley et al. (1996) demonstrated for instance that the amount of paramagnetic iron minerals is linearly correlated with the NMR relaxation rate for materials with otherwise identical pore space. Keating and Knight (2007, 2010) found that NMR relaxation is not only influenced by the amount but also by the specific kind of iron oxide mineral. Additional complexity might occur if paramagnetic and ferromagnetic particles accumulate inhomogeneously inside the pore space (Grunewald and Knight, 2011; Keating and Knight, 2012).

In this study, we investigate the effects of paramagnetic iron oxide coatings particularly for coarse material. For large pores in the so-called slow diffusion regime, the otherwise linear relationship between relaxation time and pore size is disturbed because higher relaxation modes become relevant (Brownstein and Tarr, 1979; Müller-Petke et al., 2015). As a significant consequence, the common interpretation schemes to estimate pore size and hydraulic conductivity are not valid anymore. Past studies dealing with iron mineral coatings reported the occurrence of slow diffusion conditions during their NMR experiments (Keating and Knight, 2010; Grunewald and Knight, 2011). Our objective is to learn how to interpret NMR data also under these conditions and how to estimate hydraulic parameters from it. Therefore, the goals of this study are:

1. to investigate the NMR relaxation behaviour as function of the content of paramagnetic iron oxide for large pores.
2. to correlate NMR relaxation parameters with hydraulically effective parameters.
3. to assess the model published by Müller-Petke et al. (2015) in the context of iron coated sediments, which is the first NMR interpretation approach that considers higher relaxation modes.

~~we solely deal with paramagnetic iron coatings, due to their abundance and importance.~~ We investigate two different sets of iron oxide-coated samples. The first set consists of commercially available filter sand that was coated with different amounts of synthetic ferrihydrite and goethite. Using this set (Set A) we study the general impact of increasing iron concentration on the NMR relaxation behaviour and investigate how sensitive the measured NMR signature is with regard to the mineral type. The second set consists of filter sand and gravel with natural iron oxide incrustations and material taken from the clogging experiments of Weidner (2016), who investigated the influence of chemical iron-clogging on the hydraulic conductivity of gravel pack material in a sandtank model. The iron oxide content of these samples consists of different amounts of ferric oxide minerals, including ferrihydrite and goethite. Using this set (Set B), we ~~analyse~~ test the general potential of NMR to provide a reliable proxy for hydraulic conductivity even with the content of individual paramagnetic iron oxides varying arbitrarily.

2 Basics of NMR relaxation in porous media

2.1 Principle of NMR relaxometry

The measurement principle is based on the manipulation of hydrogen protons (e.g. in water molecules). They exhibit a magnetic momentum due to their proton spins. When an ensemble of proton spins is exposed to a permanent magnetic field $\boldsymbol{B_0}$, an additional (nuclear) magnetisation $\boldsymbol{M}$ is formed and aligned with $\boldsymbol{B_0}$. By electromagnetic stimulation (excitation) using an external field $\boldsymbol{B_1}$ that alternates the Larmor frequency of proton spins, $\boldsymbol{M}$ can be forced to deflect from its equilibrium position. After shutting off the excitation, the movement of $\boldsymbol{M}$ back to equilibrium is observed. This process is called NMR relaxation and the resulting signal, recorded as induced voltage in a receiver coil, is an exponential decrease (transverse or T_2-relaxation) when measured perpendicular to $\boldsymbol{B_0}$. When observed parallel to $\boldsymbol{B_0}$, the signal increases correspondingly (longitudinal or T_1 relaxation). Detailed information on theory and measurement techniques is found in e.g. Coates et al. (1999) and Dunn et al. (2002).

2.2 NMR relaxation in general

Because only the hydrogen proton spins of the pore water molecules contribute to the NMR signal, its amplitude is a measure for the water content of the investigated material, while the relaxation behaviour encodes relevant information on the pore environment. The NMR signal E (in V) ~~(in V)~~ as function of the measurement time t is described by

$$E(t) = E_0 \left[1 - \sum_n I^n \exp\left(-\frac{t}{T_1^n}\right)\right] \quad (1)$$

and

$$E(t) = E_0 \sum_n I^n \exp\left(-\frac{t}{T_2^n}\right) \quad (2)$$

for the T_1 and T_2 relaxation, respectively. E_0 is the initial amplitude (in V) ~~(in V)~~, while I^n and T_i^n (i = 1, 2) denote the relative intensity (no units) and relaxation time (in s) of the n-th relaxation regime.

When considering the T_1 relaxation, the relaxation rate $1/T_1^n$ is given by

$$\frac{1}{T_1^n} = \frac{1}{T_{1,bulk}} + \frac{1}{T_{1,surf}^n} \quad (3)$$

where $1/T_{1,bulk}$ and $1/T^n_{1,surf}$ describe the relaxation rates of the pure pore water, excluding the influence of the pore walls (bulk relaxation), and the interaction of the proton spins with the pore surface (surface relaxation), respectively. For the general description of the T_2 relaxation, an additional term must be included:

$$\frac{1}{T_2^n} = \frac{1}{T_{2,bulk}} + \frac{1}{T_{2,surf}^n} + \frac{1}{T_{2,diff}} \quad (4)$$

The rates $1/T_{2,bulk}$ and $1/T^n_{2,surf}$ are the same as for the T_1 relaxation, whereas the $1/T_{2,diff}$ considers the case of an inhomogeneous $\boldsymbol{B_0}$-field. The diffusion relaxation must be taken into account, if a significant content of ferromagnetic minerals is present (Keating and Knight, 2007, 2008) or if the sensitive volume of the measurement includes a significant gradient in $\boldsymbol{B_0}$ (Blümich

et al., 2008; Perlo et al., 2013). However, for the estimation of hydraulic properties from NMR, the surface relaxation is the most interesting phenomenon.

Brownstein and Tarr (1979) derived the NMR relaxation behaviour in restricted environments for simple pore geometries (planar, cylindrical, and spherical). In this study, we consider the corresponding relaxation inside a cylindrical capillary with radius r_c, which exhibits different relaxation modes:

$$T_{i,surf}^{n} = \frac{r_c^2}{D\xi_n^2} \text{ with } \xi_n \frac{J_1(\xi_n)}{J_0(\xi_n)} = \frac{\rho_i r_c}{D}. \quad (5)$$

D refers to the self-diffusion coefficient of water (in m^2/s) and ρ_i to the surface relaxivity (in m/s) for either the longitudinal (i = 1) or the transverse (i = 2) relaxation, which is a material constant describing the influence of paramagnetic minerals at the pore surface. J_0 and J_1 are the Bessel functions of the zeroth and first order, respectively. The quantities ξ_n can only be found by calculating the positive roots of the corresponding equation numerically. The intensities I^n are given by

$$I^n = \frac{4J_1^2(\xi_n)}{\xi_n^2[J_0^2\xi_n + J_1^2(\xi_n)]}. \quad (6)$$

According to Brownstein and Tarr (1979), the term $\rho_i r_c/D$ in Eq. 5 defines a controlling criterion that distinguishes between the fast ($\rho_i r_c/D << 1$), intermediate ($1 < \rho_i r_c/D < 10$), and slow ($\rho_i r_c/D > 10$) diffusion regimes. Figure 1a and b demonstrate the relative intensities I^n of the zeroth to third modes as functions of $\rho_i r_c/D$ for all diffusion regimes. Obviously, the zeroth mode I^0 is the only relevant relaxation component taking place in the fast diffusion range, because the intensities of the higher modes can be neglected, i.e. the relaxation is mono-modal inside the considered pore. The phenomenological explanation for this feature is that all proton spins in the pore space diffuse fast enough to sample the entire pore surface during the NMR relaxation measurement, which is the case for small pores and low surface relaxivities. Only if this condition is satisfied, the common empirical approaches to provide hydraulic conductivity estimates (e.g. Kenyon, 1997; Coates et al., 1999; Knight et al., 2016) and pore size distributions (e.g. Hinedi et al., 1997; Costabel and Yaramanci, 2013) are valid: the zeroth mode in Eq. 5 simplifies to $T_{i,surf}^{0} = r_c/2\rho_i$ and, given that ρ_i can be determined by calibration, becomes a unique proxy for a certain pore (capillary) radius.

Outside the fast diffusion regime, the intensities I^n for $n > 1$ increase (Figure 1a and b), while I^0 decreases asymptotically to about 0.7. In materials with large pores and/or high surface relaxivities, the self-diffusion of the proton spins is slow in regard to the mean distance to the pore surface and thus, the excited protons do not equally get in touch with the pore surface. Protons in the direct vicinity of the surface exchange their spin magnetisation faster than those within the pore body. The consequence is a multi-exponential (i.e. multi-modal) relaxation inside the pore. The theory of Brownstein and Tarr (1979) leads to the simplification of $\xi_n = (n + 1/2)^2\pi^2$ in Eq. 5 describing the asymptotic behaviour in the slow diffusion regime. This is in principle a significant advantage regarding the estimation of pore radii from relaxation times, because a calibration regarding ρ_i is not necessary. However, natural unconsolidated sediments exhibit a large range of pore sizes, which are seldom completely in the slow diffusion regime. Thus, a close description of the problem is desired that considers all diffusion regimes at once.

~~**2.3 Special cases of relaxation**~~

~~Under fast diffusion conditions, the zeroth mode ($n = 0$) of the surface relaxation defined in Eq. 5 is the only component and simplifies to (Brownstein and Tarr, 1979):~~

$$~~T^{0}_{1,surf} = \frac{r_c}{2\rho_1}~~ \quad ~~(7)~~$$

~~In this case, the relaxation time $T^{0}_{1,surf}$ is a proxy for the pore radius and the multi-exponential approximation of the NMR relaxation measurement according to Eq.s 1 and 2 can be treated as an estimate of the pore radius distribution with the relative intensities being the volumetric portions of each characteristic pore size (Kenyon, 1997; Hinedi et al., 1997; Costabel and Yaramanci, 2013). However, to identify the pore size information from NMR relaxation times, calibration regarding ρ_1 is necessary to overcome the ambiguity in Eq. 7.~~

~~Under slow diffusion conditions, i.e. when the zeroth mode has reached the asymptote for large $\rho_1 r_c/D$ (see Figure 1a), ξ_n simplifies to $(n + 1/2)^2\pi^2$ (Brownstein and Tarr, 1979). In this case, the relaxation times in the slow diffusion regime do not depend on ρ_1 any more, which is in principle a significant advantage regarding the estimation of pore radii from relaxation times. However, natural unconsolidated sediments exhibit a range of pore sizes and are, therefore, seldom completely in the slow diffusion regime. Thus, a close description of the problem is desired that considers all diffusion regimes at once. Godefroy et al. (2001) found an analytical solution valid for all diffusion regimes for the particular relaxation rate of the zeroth mode (i.e. $n = 0$):~~

$$~~T^{0}_{1,surf} = \frac{r_c}{2\rho_1} + \frac{r_c^2}{4D}~~ \quad ~~(8)~~$$

~~However, Eq. 8 still demands a calibration regarding ρ_1 and is not able to take advantage of the direct sensitivity of the relaxation times to the pore radius outside the fast diffusion regime.~~

2.~~4~~ 3 Analysis of relaxation modes

The pore space of a well-sorted porous material has a narrow pore size distribution that can be described using a single effective pore radius (r_{eff}). For this case, Müller-Petke et al. (2015) showed that the consideration of relaxation modes as defined in Eq.s 5 and 6 leads to an unambiguous prediction of pore radius and surface relaxivity in the intermediate diffusion regime. In this study, we use this concept to interpret, i.e. to approximate, our NMR relaxation measurements. As demonstrated in the following section, the investigated sample material in this study allows the assumption of a single r_{eff} to describe the pore space. We accept the ~~In doing so, we accept the~~ limitation on a single effective pore radius ~~of one single r_{eff} to describe the pore space of the investigated material~~ for the benefit of a closed model that includes the relaxation modes outside the fast diffusion regime on the one hand and that does not demand a priori information on the diffusion regime or calibration of ρ_1 on the other.

However, depending on the actual diffusion regime of the sample, the performance of the approximation procedure as well as the general results differ significantly. To demonstrate the corresponding effects, we calculated the synthetic T_1 relaxation

response signals according to Eq.s 1, 5, and 6 for a cylindrical pore with a radius r_c = 100 µm and surface relaxivities ρ_1 = 20, 200, 2000 µm/s. The positions of these three parameter combinations in Figure 1a and b show that they represent one specimen for each relevant setting of the relaxation modes: the first at $\rho_i r_c/D$ = 1, where I^0 is close to one, the second at $\rho_i r_c/D$ = 10, where the corresponding I^0 lays inside the decreasing range; and the third at $\rho_i r_c/D$ = 100, where I^0 has reached the asymptote. The initial amplitudes E_0 of the synthetic signals were set to one and the resulting synthetic signals are exposed to a Gaussian distributed noise with an amplitude of 0.01 (Figures 1c to e).

Figures 1f to h show the results of a parameter search for each of the three cases as surface plots (i.e. their objective functions), where the surface height demonstrates the relative root mean square value (rms) of each combination of ρ_1 and r_c within the search region. The black region in each figure demonstrates the area, where the resulting rms value is 0.01, i.e. where the corresponding parameter combinations lead to a reliable approximation of the original signal within its noise level. According to the findings of Müller-Petke et al. (2015), a unique solution for both parameters can only be found for the signal at $\rho_i r_c/D$ = 10 (Figure 1g). The fast diffusion regime in Figure 1f is characterised by an ambiguous region demonstrating the linear relationship of ρ_1 and r_c, while the solution of the third signal at $\rho_i r_c/D$ = 100 is independent of ρ_1 (Figure 1h). Two important facts can be deduced from Figure 1h: first, by performing a parameter search for NMR relaxation measurements under very slow diffusion conditions, only a minimum of ρ_1 can be determined, and, second, an adequate approximation algorithm based on the mode interpretation of NMR relaxation will always provide a reliable estimate of r_c outside the fast diffusion region, while the corresponding ρ_1 estimate becomes more and more inaccurate when passing through the slow diffusion regime.

In contrast to ferromagnetic impurities that mainly affect the diffusion relaxation by small-scaled disturbances of the magnetic fields involved, the appearance of purely paramagnetic iron mineral coatings is expected to cause an increase in ρ_i and thus a faster relaxation (e.g. Foley et al., 1996; Keating and Knight, 2007). However, iron oxides are known to have large surface areas (e.g. Houben and Kaufhold, 2011) and will consequently affect the NMR relaxation also by an increasing pore surface-to-volume ratio *S/V* (Foley et al., 1996~~; Hinedi et al., 1997~~; Müller-Petke et al., 2015). It is generally impossible to relate an observed increase in NMR relaxation unambiguously to either an increase in ρ_i or to an increase in *S/V* without additional information. Along with the general behaviour of relaxation modes, numerical modelling of Müller-Petke et al. (2015) demonstrated that an increasing roughness of the surface inside a capillary with otherwise low and constant ρ_i leads to a similar relaxation as an increasing surface relaxivity, while keeping the radius unchanged. They introduced and defined the apparent surface relaxivity $\rho_{i,app}$ in combination with an apparent pore radius r_{app}^{NMR} to explain NMR relaxation of porous media with narrow pore size distribution. Following their suggestion, we define $\rho_{i,app}$ to include both the effect of an increasing ρ_i and the corresponding increase of pore surface roughness due to iron oxide coating, while r_{app}^{NMR} is considered to be the mean radius of the corresponding capillary. ~~They suggested the consideration of an apparent surface relaxivity $\rho_{i,app}$ in combination with an apparent pore radius r_{app}^{NMR} to explain the NMR relaxation of porous media with narrow pore size distribution and link it to hydraulic properties. Following this logic, we hypothesise that $\rho_{i,app}$ includes both the effect of an increasing ρ_i and the corresponding increase of pore surface roughness, when dealing with paramagnetic iron oxide coating.~~ The hypothesis

demands the assumption that the coating and the corresponding distribution of $\rho_{i,app}$ is homogeneously distributed. This is a crucial point, because a perfect~~ly~~ homogeneous distribution of iron precipitation at the pore scale due to natural chemical or microbiological processes or even synthetic chemical treatment is questionable. However, regarding the slow NMR relaxation in coarse sediments it is expected that, during the NMR measurement, the diffusing spins statistically sample possible inhomogeneities in the distribution of ρ_i or $\rho_{i,app}$ inside the pore space uniformly enough to allow the assumption of a mean surface relaxivity (Kenyon, 1997; Grunewald and Knight, 2011; Keating and Knight, 2012). An important objective of this study is the comparison of $r_{app}{}^{NMR}$ with the effective hydraulic pore radius r_{eff}.

3 Material and methods

3.1 Samples with controlled synthetic ferrihydrite and goethite coating

In the first experimental step, the focus was set on a simplified binary system consisting of (a) a relatively uniform carrier phase, quartz in the form of commercially available filter gravel, and (b) synthetically produced iron oxides. For the latter, ferrihydrite and goethite mineral phases were studied separately, both of which are common constituents in soils and aquifers but also in incrustations. Synthetic iron oxides were used because of their controlled crystallite size and composition (Schwertmann and Cornell, 2000). Ferrihydrite is a poorly crystalline mineral that usually precipitates as the first stable oxidation product when dissolved ferrous iron comes into contact with oxygen. Since ferrihydrite is thermodynamically meta-stable, it will convert over time into the more stable goethite (e.g., Houben and Kaufhold, 2011). This process is strongly accelerated at higher temperatures (> 50°C) and involves a significant reduction of specific surface area and therefore water content, density and chemical reactivity. Thus, this study does not only encompass two of the most important iron oxides but, at the same time, two different stages of crystallinity, age and reactivity.

Two series of artificially coated filter sand samples (Set A) were prepared by precipitating the Fe(III)-minerals ferrihydrite and goethite onto quartz following Böhm (1925) and Schwertmann and Cornell (2000). Therefore, iron nitrate nonahydrate ($Fe(NO_3)_3 \cdot 9\ H_2O$; CAS: 7782-61-8, technical purity, BDH Prolabo) was dissolved in twice de-ionised water to attain a 1 mol/L solution. A 5 mol/L potassium hydroxide solution (KOH, CAS: 1310-58-3, Bernd Kraft) was used to trigger precipitation of ferrihydrite ($Fe_5HO_8 \cdot 4\ H_2O$). The desired contents of iron in the filter sands were realised by varying the amounts of the two solutions, added to a fixed amount of filter sand. After precipitation the residual solution was carefully exchanged by washing with de-ionised water. For transformation of ferrihydrite to goethite (α-FeOOH), a second batch of ferrihydrite was held in a closed glass bottle at 70 °C for 60 hours. The applied recipes for ferrihydrite and goethite are based on the collection of standard synthesis procedures compiled in the reference book by Schwertmann and Cornell (2000). They have been successfully applied in numerous studies (e.g. Janney et al., 2000; Houben 2003b; Houben and Kaufhold 2011).

After preparation, the sample material was filled into circular petri dishes with a diameter of 50 mm and a height of 15 mm to perform the initial NMR measurements. Most of the iron particles settled to the bottom and formed a gradient in iron

concentration inside the dishes, which could visually be observed for most of the samples due to an obvious increase of reddish colour from top to bottom. Initial NMR measurements were performed to qualitatively analyse the vertical distribution of the iron content. Therefore, measurements at different heights of the sample holders were conducted. However, for the quantitative analysis of NMR parameters, the samples were homogenised before the final NMR measurements, because it was not possible to determine the amount of iron as a function of height inside the sample holders by chemical analyses. To homogenise the iron content inside the petri dishes, the material was exposed to the atmosphere for one day, where it evaporated to a certain state of partial saturation (resulting saturation: 0.2 to 0.5), mixed, and filled into dishes with a diameter of 50 mm and a height of 10 mm. Afterwards, samples were dried completely to ensure a proper coating of the pore walls with the iron particles. To maintain a homogeneous iron distribution throughout the sample and a better adhesion to the quartz surface, the material was moistened (de-ionised water) and dried out again. This procedure was repeated four times for each sample. Finally, the samples were completely saturated with de-ionised water prior to the NMR measurements.

After the final NMR measurements, the samples were air-dried again to determine their porosity Φ by weight. Afterwards they were subdivided for the controlling analysis. The iron content of each sample was analysed chemically to identify whether and to what extent the precipitation had led to the desired results. This was done by ~~first~~ analysing the amount of dithionite-soluble iron, following the method of Mehra and Jackson (1960). The oxidic iron coatings that are expected to affect the NMR results are re-dissolved with dithionite solution and quantified by measuring the iron concentration in the solution. The total iron content was investigated by X-ray fluorescence analysis (XRF, using a PANalytical Axios and a PW2400 spectrometer) for verification. The latter method is expected to yield slightly higher iron contents, because XRF also captures the iron content bound in silicates of the filter sand or gravel grains. ~~However, due to the high proportion of quartz, contents of siliceous iron are generally expected to be very low in fresh filter sands.~~ The grain size distributions ~~was~~ were determined using a Camsizer (Retsch GmbH). The specifications of the samples are summarised in Table 1. The comparison of the desired with the actually achieved Fe-contents indicates that, during the exchange of the remaining synthesis solutions ($Fe(NO_3)_3$ and KOH) with H_2O_{dest}, some of the fine precipitates have been washed out. The difference for the samples of Set A indicates an amount of siliceous iron in the range of 0.5 to 0.7 g/kg. The further analysis is thus based on the actually measured ~~Fe~~ contents of dithionite-soluble iron ~~rather than the desired ones~~. A part of each sample was also prepared for the determination of the specific surface area using the BET method (Brunauer et al., 1938). However, the corresponding results fell below the accuracy limit of the device and are not reliable. Obviously, the contents of iron oxide in the investigated samples are too small and the surface area is still dominated by the quartz grains.

3.2 Samples with natural iron coating

A second set of samples with natural iron coatings was also studied (Set B, Table 2). This set consists of gravel samples from laboratory well clogging experiments (Weidner, 2016), but also encrusted filter sand and gravel samples taken from excavated wells. The analyses were the same as for Set A.

3.3 Estimation of effective pore radius and hydraulic conductivity from grain size distribution

To obtain consistent reference values for comparison with the NMR results, we estimated the effective pore radius from the effective grain diameter d_{GSD} as defined by Carrier (2003), who suggested the use of the equations of Kozeny (1927) and Carman (1939) to estimate the hydraulic conductivity from grain size distribution (GSD) data:

$$d_{GSD} = \left(\sum_i \frac{f_i}{\sqrt{D_{li} D_{ui}}}\right)^{-1} \quad (97)$$

where f_i refers to the i-th weight fraction of grains within the respective sieve size limits D_{li} and D_{ui} with $\Sigma_i f_i = 1$.

To estimate the effective pore radius r_{eff} from d_{GSD}, we determine the ratio of the wetted surface and the pore volume (= specific surface) for both the capillary geometry of our pore model and the spherical geometry assumed for the effective grain diameter:

$$\frac{pore\ surface}{pore\ volume} = \frac{2\phi}{r_{eff}} = \frac{6(1-\phi)}{d_{GSD}} \quad (108)$$

with ϕ being the porosity. The effective pore radius is then given by:

$$r_{eff} = \frac{1}{3}\frac{\phi}{1-\phi} d_{GSD}. \quad (119)$$

The Kozeny-Carman equation, when considering a cylindrical capillary with effective radius r_{eff}, is defined as (e.g. Pape et al., 2006):

$$K_{KC} = \frac{\varrho g}{\eta}\frac{1}{8\tau}\phi r_{eff}^2. \quad (1210)$$

The parameter τ refers to the tortuosity (no units), g to the gravity acceleration (9.81 m/s^2), and ϱ and η to the density (1000 kg/m^3) and dynamic viscosity (0.001 kg/(m·s)) of the pore water, respectively. The tortuosity is set to 1.5 in this study, which is a reliable estimate for coarse sand and gravel (e.g. Pape et al., 2006; Dlugosch et al., 2013).

An alternative to the semi-empirical Kozeny-Carman equation is the well-known empirical formula of Hazen (1892). The effective measure in this approach is assumed to be the grain diameter corresponding to the 10-wt% percentile of the cumulative GSD (d_{10}). The corresponding estimates of hydraulic conductivity K_{Hz} were used as an additional set of reference values.

3.4 NMR measurements

As described above in section 3.1, the stimulated precipitation yielded an obvious vertical gradient in iron oxide content. To identify the corresponding level of heterogeneity and to control and verify the homogeneity of the iron oxide distribution after the final mixing, an NMR device ~~measurements were performed~~ with vertical sensitivity, i.e. the ability to apply distinct measurements at different heights of the sample holder had to be applied. ~~before and after mixing the sample material.~~ Using a common NMR Core analyser, the entire specimen is measured at once, which can lead to a misinterpretation if different relaxation regimes overlap. Therefore, the experiments in this study ~~This was~~were realised using~~by~~ a single-sided NMR apparatus (NMR Mouse, Magritek) with strong sensitivity to vertical ~~variations~~ changes inside the sample (Figure 2). Four permanent magnets for the $\boldsymbol{B_0}$ and the measurement coil for the $\boldsymbol{B_1}$ field are arranged in a way that the sensitive volume is as a

slice with a thickness of 200 µm and a footprint of about 40 by 40 mm (Kolz et al., 2007; Blümich et al., 2008). The operating frequency is 13.05 MHz. The sample is placed on a table, while the sensor is mounted on a platform adjustable in height, i.e. to move the sensitive volume over the sample (along the z-axis) with an accuracy of a few µm.

Although homogeneous in the plane parallel to the $\boldsymbol{B_1}$ coil, the $\boldsymbol{B_0}$ field strength decreases with increasing distance to the magnets, which yields a strong $\boldsymbol{B_0}$ gradient~~the $\boldsymbol{B_0}$ field strength exhibits a strong gradient~~ in the z-direction (mean gradient according to user's manual: 273 kHz/mm) inside the sensitive slide. Consequently, the T_2 measurements (CPMG sequence, for details please see Coates et al. (1999) and Dunn et al. (2002)) are dominated by the diffusion relaxation rate. In principle, this effect can be corrected to identify the proportion of surface relaxation in the data (Keating and Knight, 2008). However, testing and discussing the quality and potential of the additional measurements and calculations necessary for this correction are beyond the scope of this paper. Thus, we use the T_2 measurements only for determining the NMR porosity Φ_{NMR} from the initial amplitude of the corresponding exponential decay. Due to the linearity between NMR signal and water content inside the sensitive volume of the measurement (e.g. Costabel and Yaramanci, 2011; Behroozmand et al., 2014), Φ_{NMR} can simply be determined by the ratio of the initial amplitude of the investigated sample and that of pure water in a sample holder with exactly the same dimensions. The CPMG measurements were conducted with an echo time of 66 µs, while the total number of echos was varied individually between 3000 and 9000. The corresponding measurement times vary in a range of about 0.2 to 0.6 s.

For investigating the impact of the iron oxide coating, we use the T_1 relaxation, which is unaffected by gradients in $\boldsymbol{B_0}$. These measurements are realised as saturation recovery (SR) measurements (details see Coates et al. (1999) and Dunn et al. (2002)). Each record consists of 50 single recovery times, which are logarithmically spaced along the measurement time axis. The exact positioning of the recovery times was adjusted for each sample to realise a similar distribution of time samples from zero to equilibrium nuclear magnetisation, which was estimated beforehand by screening SR measurements with a reduced number of time samples (15) and stacks. The maximum observation time for the final SR measurements was set five times higher than the prior T_1 estimates. For each sample, SR measurements at different heights were conducted using 1-mm steps in range of z = 3 to 15 mm before and z = 3 to 10 mm after homogenisation~~For each sample, eight SR measurements at different heights were conducted (1-mm steps in the range of z = 3 to 10 mm)~~. In this way, the vertical distribution of iron inside the samples before homogenisation and the natural scattering of the NMR parameters after homogenisation were taken into account. For the latter, mean values and double standard deviations (95 % confidence interval) were calculated from the measurements at different heights. After the T_1 measurements, a small sample of pore water (a few tenths of ml) was extracted from the samples using a pipette in order to measure T_{bulk}. In some cases the extracted amount of pore water was not high enough to achieve a sufficient signal-to-noise ratio for an accurate NMR measurement. However, the T_{bulk} values of the successful measurements did not vary significantly among the samples. Consequently, for the analysis of the relaxation behaviour (Eq. 3) we use a mean T_{bulk} (2.46 ms ± 0.07 ms) for all samples.

Because the NMR porosity was determined from the T_2 measurements, it was not necessary to take the initial amplitude of the T_1 measurements into account. Thus, each SR time series was normalised to 1 prior to the final signal approximation. Although the main focus of our interpretation is on the approximation using the relaxation modes, we also fitted the data using the

commonly used multi-exponential spectral inversion for comparison. As an example, Fig. 3a shows all T_1 measurements of the homogenised sample F4, i.e. all repetitions at different heights, and their approximations using the spectral approach. The corresponding spectra, depicted in Fig. 3b, demonstrate that the probability functions of all repeated T_1 data are in good agreement. They show a dominating peak with a maximum at about 1.3 s and a smaller peak around 0.1 s.

3.5 Testing for NMR diffusion regimes

The analysis of relaxation modes is useful only outside the fast diffusion regime. Thus, the question arises how the diffusion regime can be tested in practice. According to Kenyon (1997), the diffusion condition inside a pore is defined by the ratio of the time for a proton spin to diffuse across the pore (= r_c^2/D) and the surface relaxation time:

$$\kappa = \frac{r_c^2/D}{T_{i,surf}^{0}} \quad (13\,11)$$

which leads to the same theoretical criterion as already given by Eq. 5, when combined with Eq. 7 (except of the factor of two, which is a result of the consequent consideration of a cylindrical pore shape). Using the logarithmic mean of the measured relaxation spectra $T_{1,lm}$, the self-diffusion coefficient of water, and accepting r_{eff} as a reliable estimate of r_c, we combine Eq. 13 11 with Eq. 3 to determine a measure that can be used for practical testing of the diffusion regime:

$$\kappa \approx \frac{r_{eff}^2/D}{(T_{1,bulk}T_{1,lm})/(T_{1,bulk}-T_{1,lm})}. \quad (14\,12)$$

3.6 Inversion of NMR relaxation modes

The uniformity coefficient is defined by the ratio of the grain diameters corresponding to the 60- and 10-wt% percentile of the cumulative GSD. For all samples investigated in this study it is very low (i.e. < 5, see Tables 1 and 2), which indicates a narrow grain size and consequently narrow pore size distribution (see also the supplemental Figure S1). Thus, the precondition to use the approach of Müller-Petke et al. (2015) (see Section 2.3) to fit and interpret the NMR data is fulfilled. The approximation algorithm, i.e. the data inversion yielding the relaxation modes

1. starts using an initial model with given $\rho_{1,app}$ and r_{app}^{NMR},
2. calculates the corresponding multi-exponential NMR response by solving Eq.s 3, 7 5 and 8 6,
3. compares the result with the measured NMR signal by means of least squares,
4. modifies the parameters $\rho_{1,app}$ and r_{app}^{NMR} if necessary, that is if the modelled response and the measurement do not coincide, and
5. repeats the procedure until an optimal parameter set $\rho_{1,app}$ and r_{app}^{NMR} is found that explains the data.

We use the nonlinear solver lsqnonlin of the Matlab(R) optimization toolbox (MATLAB®, 2016) for this processing step. Figure 3c shows the same data as Fig. 3a, but together with the approximations resulting from relaxation modes inversion that obviously lead to identical fits compared to the spectral inversion. Figure 3d shows the corresponding results in the I^n-T_1-

domain, that is, the first 10 modes for each measurement as separate spectral lines. The accuracy of the approximations using the relaxation modes represented by the corresponding rms values are similar to the ones of the spectral inversion.

4 Results and discussion

4.1 NMR-based porosity measurements

As mentioned above, to determine Φ_{NMR} of a sample, an additional NMR measurement using pure water is necessary. Figure 4a shows the T_2 data of sample F4 (synthetic ferrihydrite on quartz) and pure water. Due to the diffusion relaxation, the latter exhibits a relaxation time of less than 0.2 s, which is much shorter than that usually measured for water (2 – 3 s) in a homogeneous $\boldsymbol{B_0}$. Because the initial signal amplitudes are not affected by the $\boldsymbol{B_0}$ gradient, Φ_{NMR} can nevertheless be estimated from the T_2 data. Figure 4b shows the NMR-based porosities of all samples after homogenisation compared to those measured by weight. The NMR porosities coincide with the reference values within their uncertainties, which are determined as doubled standard deviations (95 % confidence interval) of the measurement repetitions at different sample heights. However, the uncertainties of the Φ_{NMR} estimates measured using the single-sided NMR device in this study are larger than those of past studies, where conventional laboratory NMR techniques are applied (e.g. Costabel and Yaramanci, 2011; Behroozmand et al., 2014). The reason for this is the relatively thin~~small~~ sensitive slide of 200 µm~~volume,~~ in combination with the investigated coarse material exhibiting mean r_{eff} values of 95 to 474 µm (see Table 1 and 2). The inaccuracy of the porosity estimates must be accepted as a natural consequence of the fact that some of the observed pores exceed the z-dimension of the probed reference volume (e.g. Costanza-Robinson et al., 2011).~~(mean grain size about 1000 µm, see Table 1). By probing a thin slide of 200 µm, the mean porosity of the entire sample is not captured. Thus, a larger natural scattering of porosity values measured at different sample heights must be accepted.~~

4.2 The logarithmic mean of relaxation as qualitative measure for iron content at the pore walls

A photograph of sample F4 after the ferrihydrite precipitation is shown in Fig. 5a. The reddish section indicates that most ferrihydrite particles settled at the bottom of the petri dish. The same phenomenon was optically observed for almost all samples of Set A. Even though this separation was not visibly apparent in samples F1, F2 and G2 with the highest iron contents, we still expected a gradient in the iron content with z-direction for these samples as well. Although not quantifiable to date, it is expected that the mean NMR relaxation time depends on the amount of paramagnetic iron oxides in the pore space (Keating and Knight, 2007). Thus, we performed initial NMR measurements (T_1 and T_2) to qualitatively analyse the level of inhomogeneity in the vertical ferrihydrite and goethite distributions by comparing the NMR parameters at different heights over the sample holders. Figure 5b and c depict the NMR data of sample F4 and those of the pure uncoated filter sand (sample S0), that is, the corresponding porosity determined from the E_0 amplitude of the CPMG data and the distributions of the logarithmic mean relaxation times ($T_{1,\,lm}$ and $T_{2,\,lm}$), respectively. Apart from a decrease at the top, the porosity distributions of both samples are homogeneous. It is likely that the decrease at the top is caused by evaporation caused by an imperfect sealing

of the sample. The same feature was observed for all samples of Set A to varying extent. Figures ~~S1~~S2-~~S14~~ S16 (supplement to this paper) show the photographs of all samples compared to the corresponding distributions of porosity and mean relaxation times. Some of the samples also show a significant decrease in porosity at the bottom of the sample holder, which is caused by small iron oxide particles accumulating in the voids between the quartz grains.

Whereas both the $T_{1,\,lm}$ and $T_{2,\,lm}$ distributions of the uncoated sample S0 appear to be homogeneous throughout the z-axis, the general trend in the distributions of sample F4 is a gradual decrease from top to bottom (Figure 5c), indicating the increase in surface relaxation with increasing ferrihydrite content. The difference between T_1 and T_2 is about one order of magnitude, which is caused by the high diffusion relaxation rate in the inhomogeneous $\boldsymbol{B_0}$-field of the single-sided NMR apparatus, as expected (see Section 3.4). When comparing the $T_{1,\,lm}$ and $T_{2,\,lm}$ curves of F4 with S0, it seems that no ferrihydrite remains at the top, because here the curves of both samples are almost in agreement. Although we cannot quantify the ferrihydrite content as function of z by chemical analyses, we note that the logarithmic means of both T_1 and T_2 are qualified proxies for the corresponding iron content distributions.

To relate the measured NMR parameters with the iron content, the samples had to be homogenised (see Section 3.1). Obviously, both the $T_{1,\,lm}$ and $T_{2,\,lm}$ distribution of the homogenised F4 sample are almost constant with z (Figure 5 d to f). The $T_{1,\,lm}$ values of F4 are generally smaller than the ones of S0. In contrast, the $T_{2,\,lm}$ distributions of F4 and S0 are almost identical, which is due to the influence of the high diffusion relaxation that masks the impact of the ferrihydrite content on the surface relaxation. As for the inhomogeneous sample, the porosity distributions of F4 and S0 are almost identical, i.e. an obvious impact of the increased content of ferrihydrite on the porosity is not observed. The process of homogenisation was applied and controlled for each sample of Set A. The supplemental Figures ~~S15~~ S17 – ~~S28~~ S31 show the corresponding distributions of porosity and mean relaxation times as functions of sample height for all samples. The remaining scattering of the z-dependent NMR parameters is considered as uncertainty intervals depicted by error bars (95% confidence intervals) in the following analysis.

In Figure 6, we show the relaxation time spectra of all samples of Set A and their corresponding mean values as a function of iron content. The principle trend is the same for both minerals. For iron contents smaller than approximately 0.7 g/kg, the main peak (between approximately 0.5 and 4 s) does not change significantly, whereas the logarithmic mean slightly decreases with increasing iron content in the same range. This increase is caused by an increase of the smaller peak (between approximately 0.05 and 0.2 s). If the iron content increases further to values of 1 g/kg and higher, the main peak shifts towards shorter times, while the increase of the smaller peak continues. Considering the classical interpretation of NMR relaxation spectra, it is not clear at this point if the described changes of the spectra with increasing iron content are caused by an increasing amount of small pores (possibly within the iron minerals at the pore walls), by enhanced surface relaxivity (due to the increasing amount of paramagnetic coating) or by a combination of both. However, because all samples, including the initial iron-free sand, are outside the fast diffusion regime (see Table 3), we must also consider that the increase of the smaller peak might be due to the increasing occurrence of the higher relaxation modes. Since it is not possible to distinguish between the existence of relaxation modes and different pore sizes when considering the spectral approximation approach, we analyse the relaxation modes in the

next section by considering a bundle of capillaries with identical pore radius (= apparent pore radius r_{app}^{NMR}, see details in Section 2.43). This assumption is acceptable because the grain size distribution and consequently also the pore size distribution is narrow for the well-sorted materials studied here, which is proven by their small uniformity coefficient d_{60}/d_{10} (see Table 1 and 2). ~~This coefficient is defined by the ratio of the grain diameters corresponding to the 60- and 10-wt% percentile of the cumulative GSD.~~

4.3 The relaxation modes as quantitative measure for iron content at the pore walls

The relaxation mode inversion was performed for all T_1 data of Set A and B samples. When considering the relaxation modes (see Section 2.43), the underlying model consists of the apparent pore radius r_{app}^{NMR} of a virtual capillary with circular cross section and a rough surface, the NMR sink rate of which is described by the apparent surface relaxivity $\rho_{1,app}$ (Müller-Petke et al., 2015). The corresponding r_{app}^{NMR} and $\rho_{1,app}$ results for Set A are presented in Figure 7a and b, respectively. All results of the individual measurements for each sample (= measurement at different heights) are depicted in order to avoid error bars in the logarithmic plot. We note that r_{app}^{NMR} generally tends to smaller values for increasing iron content. However, the trend is only obvious for the iron contents higher than 0.5 g/kg. At least for the ferrihydrite series, the r_{app}^{NMR} values even increase slightly for small iron contents, whereas the r_{app}^{NMR} of the goethite series remains more or less constant. The reason for this variation is likely due to the repacking of the samples after iron oxide precipitation. Considering an initially homogeneous porosity before iron precipitation, one would expect a decrease of porosity with increasing amount of iron oxide. However, due to the repacking, each sample exhibits an individual porosity. Consequently, the apparent radius, no matter if estimated by NMR or from GSD, reflects also the porosity variations, which covers the dependence on the iron content to some extent. Thus, the expected increase of r_{app}^{NMR} becomes visible only for the higher iron contents. Interestingly, the estimates of $\rho_{1,app}$ seem to be independent from the individual porosities. Figure 7b shows a monotonous increase of $\rho_{1,app}$ with iron content, at least for the samples with iron contents of < 1 g/kg. For the higher iron contents, $\rho_{1,app}$ exhibits large uncertainties, because these reach the range, where correct $\rho_{1,app}$ estimates cannot reliably be provided anymore (see Figure 1 and corresponding discussion).

It is expected that a linear dependence between the surface relaxivity and the content of paramagnetic impurities at the pore walls exists (Foley et al., 1996). To test this expectation for the apparent surface relaxivity, Figure 7c provides a focus on the data with accurate $\rho_{1,app}$ estimates, i.e. the data of samples with iron contents < 1 g/kg. The linear regression can be verified with R^2 values of 0.98 and 0.95 for the ferrihydrite and the goethite series, respectively. We note that the $\rho_{1,app}$ estimates for the goethite series are smaller than those for the ferrihydrite series by a factor of 1.85. We assume that this is an effect of the specific surface area of goethite being about up to 5 times smaller than that of ferrihydrite (goethite ≈ 20-80 m²/g vs. ferrihydrite ≈ 180-300 m²/g; ~~Stanjek and Weidler, 1992;~~ Cornell and Schwertmann, 2003; Houben and Kaufhold, 2011). The larger specific surface of ferrihydrite leads to a higher surface roughness of the pore wall coating. As explained in Section 2.43, the apparent surface relaxivity does not distinguish between the increase of the surface roughness and increase of the actual surface relaxivity due to paramagnetic impurities at the pore wall. Because both are naturally linked to each other for an iron mineral

by its individual surface area, we expect an indirect sensitivity of $\rho_{1,app}$ also on the type of iron mineral, i.e. on the composition of the iron oxide assemblage, if considering natural samples. However, to verify this assumption more iron oxides and their influence on the NMR relaxation modes must be studied in the future. Moreover, an accurate inspection of Figure 7c leads to the assumption that a slight systematic discrepancy from linearity exists for both data sets. We hypothesise that this phenomenon is also caused by the influence of the surface roughness. We have found quadratic relationships yielding regression coefficients of 1 for both data sets. However, each of our data sets consists of just five points, which is not sufficient to validate this finding. Further research is necessary to quantify the influence of the surface roughness on the apparent surface relaxivity for natural iron coatings.

4.4 Comparison of NMR-effective pore radius and hydraulic parameters

Whether the NMR-based estimates of r_{app}^{NMR} can be considered to be reliable estimates of the effective hydraulic radius r_{eff} is examined in the crossplot in Figure 8. The linear correlation between the two is verified with an R^2 of 0.58 when considering a constant offset (regression coefficient: 0.79) and 0.53 when enforcing the point [0,0] in the fitting algorithm. The regression coefficient of the latter is very close to identity with 1.02.

Figures 9 correlates r_{app}^{NMR} and the corresponding estimates of hydraulic conductivity K_{NMR} with the reference values of hydraulic conductivity K for both Sets A and B. The K_{NMR} values were estimated according to Eq. ~~12~~ 10 using the porosities determined from the T_2 measurements discussed with Fig. 4. Because measurements of K are only available for 8 samples of Set B, we use the K estimates derived from the GSD (Section 3.3) as reference values for all investigated samples, i.e. K_{KC} according to Eq. ~~12~~ 10 in Figure 9a and K_{Hz} according to Hazen (1892) in Figure 9c. For both approaches, the correlation between r_{app}^{NMR} and K is verified with an R^2 of 0.66 and 0.57, when considering a power law to describe the relation mathematically (Fig. 9a and b). The assumption of a power law is suggested by the Kozeny-Carman equation (Eq. ~~12~~10), where the exponent of the pore radius should be 2. The actual exponent for our data set reaches slightly higher values of 2.41 (K_{KC}) and 2.20 (K_{Hz}). The linear regression between K_{NMR} with K_{KC} and K_{Hz} (Fig. 9c and d) is verified with an R^2 of 0.47 and 0.38, while the corresponding regression factors are 0.85 and 2.45, respectively.

4.5 Discussion on field applicability

The relaxation analysis in this study is limited to T_1 data, the measurement of which in boreholes and on the surface is time-consuming and therefore often inefficient to date. Besides improving the performance of T_1 measurements, future research activities in the given context will also focus on T_2 relaxation measurements, which are often the preferred choice in practical applications. Considering the NMR relaxation theory, the findings of this study regarding the influence of the iron-coated pore surface on T_1 are expected to be valid for T_2 as well. However, the exact analysis of T_2 data regarding higher relaxation modes is crucial if measured in inhomogeneous $\boldsymbol{B_0}$, because the diffusion relaxation will mask the effect of the modes to some extent. This is expected to be the case for the measurement device used in this study but is also for borehole NMR (e.g. Sucre et al., 2011; Perlo et al., 2013). Moreover, the data quality of field and borehole measurements is lowered compared to laboratory

data by environmental electromagnetic noise. Future research in the framework of iron-coated soils and sediments will therefore focus on potential approaches to correct the influence of the diffusion relaxation rate caused by external field gradients and to identify and characterise the occurrence of relaxation modes in T_2 data under field conditions. However, this study demonstrates that the NMR method is principally applicable to locate and hydraulically characterise zones with iron oxides accumulation in the pore space. In addition, NMR can provide indications of a beginning iron coating by changes in the apparent surface relaxivity, even before the effective hydraulic radius decreases, i.e. before a serious hydraulic clogging takes place.

5. Conclusions

NMR relaxation data of water-saturated sand and gravel are very sensitive to the amount of paramagnetic iron oxides. Here, this is confirmed using samples with synthetic ferrihydrite and goethite coatings ~~and~~ as well as filter sand and gravel pack samples with varying contents of different natural iron oxides. We showed that the mean relaxation time can serve as robust qualitative measure for the inhomogeneous distribution of iron content inside a sample. When focusing on the quantification of NMR parameters as a function of the iron content, the inversion of NMR data considering higher relaxation modes (Brownstein and Tarr, 1979; Müller-Petke et al., 2015) turns out to be a powerful tool, as long as the NMR relaxation takes place outside the fast diffusion regime, which is true for all samples investigated in this study. ~~On the one hand, the corresponding NMR-based estimate of apparent pore radius is shown to be a reliable proxy for the effective hydraulic radius and consequently suitable for estimating hydraulic conductivity without calibration. On the other hand~~First, the inherent estimates of apparent surface relaxivity represent a qualified measure that linearly depends on the iron content, at least in the range < 1 g/kg for our data, above which the sensitivity of NMR for the surface relaxivity vanishes. However, a further increase of iron content above that limit is nevertheless indicated by a decrease of the NMR-based estimate of apparent pore radius. Second, the corresponding NMR-based apparent pore radius is shown to be a reliable proxy for the effective hydraulic radius, which was verified in this study by comparison with reference estimates from grain size distributions. An important consequence of this finding is that estimates of hydraulic conductivity can be provided from NMR outside the fast diffusion regime without any calibration.

The need for future research must be noted. Beside the limitation on intermediate and slow diffusion regimes, relaxation mode inversion as suggested in this paper is only reliable for well-sorted material with a narrow pore size distributions. Otherwise the assumption of a single effective radius might not be true. Future studies will consider the existence of both different characteristic pore sizes and higher relaxation modes. In contrast to the experimental design used here, these studies must combine NMR and direct hydraulic measurements, because broad distributions of grains can systematically bias the results of simple hydraulic models based on texture (e.g. Boadu 2000). Corresponding reference analysis regarding the pore size distribution might consist of imaging analysis or pressure-based water retention measurement.

The~~se~~ findings of this study are promising and interesting within the framework of hydraulic characterisation of aquifers or soils with significant content of paramagnetic iron oxides. The NMR method can complement other geophysical methods in

the detection of natural iron oxide accumulations, such as bog iron, laterites, iron-rich paleo soils and hardpan, provided that they are water-saturated. Moreover, a new potential application field for borehole NMR can be established: the identification and localisation of beginning iron incrustation in wells and/or the efficiency control of rehabilitation measures. Our future research activities will focus on the development of a corresponding methodology. ~~However, two significant limitations and the need for future research must be noted. First, beside the limitation on intermediate and slow diffusion regimes, relaxation mode inversion is only reliable for well-sorted material with a narrow pore size distributions otherwise the assumption of an effective radius might not be true. Future studies should consider the existence of both different characteristic pore sizes and higher relaxation modes.~~

~~Second, the relaxation analysis in this study is limited to T_1 data, the measurement of which in boreholes and on the surface is too time-consuming to be efficient to date. The exact analysis of T_2 data is crucial when measured in inhomogeneous $\boldsymbol{B_0}$, which is the case for the measurement device used in this study but is also the case for borehole NMR (e.g. Sucre et al., 2011; Perlo et al., 2013). Moreover, surface and borehole NMR work at lower operating frequencies due to lower $\boldsymbol{B_0}$ field strengths. Future research in the framework of iron coated soils and sediments should therefore focus on the use of T_2, i.e. on potential approaches to correct the influence of the diffusion relaxation rate caused by external field gradients and on the analysis of higher relaxation modes when working in lower $\boldsymbol{B_0}$ fields. However, this study demonstrates that the NMR method is principally applicable to locate and hydraulically characterise zones with iron oxides accumulations in the pore space. In addition, NMR can provide indications of a beginning iron coating by changes in the apparent surface relaxivity, even before the effective hydraulic radius decreases, i.e. before a serious hydraulic clogging takes place. Our future research activities will focus on the development of a borehole NMR based localisation and controlling system for iron oxide remediation inside wells.~~

Data availability

The NMR data at every state of processing as well as the reference data can be made available upon request. Please contact the corresponding author.

Author contribution

GH initiated and motivated the study and organised the hydrochemical treatment and reference analyses, MMP developed the software for the NMR mode inversion, CW developed and conducted the experiments for the iron oxide precipitation, and organised and characterised the sample material, SC developed and performed the NMR experiments and organised the manuscript.

Competing interests

The authors declare that they have no conflict of interest.

Acknowledgements

We thank the Institute of Hydrogeology and the Institute of Hydraulic Engineering and Water Resources Management of the RWTH Aachen University and the RWE Power AG for providing us with sample material, Stephan Kaufhold and Jens Gröger-Trampe for their advice and support on the geochemical analysis, and Raphael Dlugosch for fruitful discussions on the interpretation of the NMR data.

References

Abdel Aal, G., Atekwana, E., Radzikowski, S, and Rossbach, S.: Effect of bacterial adsorption on low frequency electrical properties of clean quartz sands and iron-oxide coated sands, Geophysical Research Letters 36, L04403, doi:10.1029/2008GL036196, 2009.

Atekwana, E. A. and Slater, L. D.: Biogeophysics: A new frontier in Earth science research, Rev. Geophys. 47, RG4004, doi:10.1029/2009RG000285, 2009.

Behroozmand, A. A., Keating, K., and Auken, E.: A Review of the principles and applications of the NMR technique for near-surface characterization, Surveys in Geophysics 36(1), 27-85, doi:10.1007/s10712-014-9304-0, 2014.

Blümich, B., Perlo, J., and Casanova, F.: Mobile single-sided NMR, Progress in Nuclear Magnetic Resonance Spectroscopy 52, 197-269, 2008.

Boadu, F.K.: Hydraulic Conductivity of Soils from Grain-Size Distributions: New Models. Journal of Geotechnical and Geoenvironmental Engineering 126 (8), 739-746, 2000.

~~Böhm, J.: Über Aluminium- und Eisenhydroxide. I. Zeitschrift für anorganische und allgemeine Chemie 149(1), 203-216, 1925.~~

Brownstein, K. R., and Tarr, C. E.: Importance of classical diffusion in NMR studies of water in biological cells: Physical Review A 19, 2446-2453, 1979.

Brunauer, S., Emmett, P. H., and Teller, E.: Adsorption of Gases in Multimolecular Layers, Journal of the American Chemical Society 60 (2), 309-319, DOI: 10.1021/ja01269a023, 1938.

Bryar, T.R., Daughney, C.J., and Knight, R. J.: Paramagnetic effects of iron(III) species on nuclear magnetic relaxation of fluid protons in porous media, Journal of Magnetic Resonance 142, 74-85, 2000.

Bryar, T.R. and Knight, R. J.: Sensitivity of nuclear magnetic resonance relaxation measurements to changing soil redox conditions, Geophysical Research Letters 29 (24), 2197, 2002.

Bryar, T.R., and Knight, R.J.: Laboratory studies of the detection of sorbed oil with proton nuclear magnetic resonance: Geophysics 68(3), 942-948, 2003.

Carman, P. C.: Permeability of saturated sands, soils and clays, The Journal of Agricultural Science 29, 262-273, 1939.

Carrier, W. D.: Goodbye, Hazen; Hello, Kozeny-Carman, Journal of Geotechnical and Geoenvironmental Engineering 129, 1054-1056, 2003.

Coates, G., Xiao, L. and Prammer, M.: NMR Logging Principles and Application, Halliburton Energy Services, Houston, 1999.

Colombo, C., Palumbo, G., He, J.-Z., Pinton, R., Cesco, S.: Review on iron availability in soil: interaction of Fe minerals, plants, and microbes, J. Soils Sediments 14(3), 538–548, DOI 10.1007/s11368-013-0814-z, 2014.

Cornell, R. M. and Schwertmann, U.: The iron oxides: structure, properties, reactions, occurences and uses. Wiley-VCH, Weinheim, 703 pp, 2003.

Costabel, S. and Yaramanci, U.: Relative hydraulic conductivity and effective saturation from Earth's field nuclear magnetic resonance – a method for assessing the vadose zone, Near Surface Geophysics 9, 155-167, doi:10.3997/1873-0604.2010055, 2011.

Costabel, S. and Yaramanci, U.: Estimation of water retention parameters from nuclear magnetic resonance relaxation time distributions, Water Resources Research 49, 2068-2079, doi:10.1002/wrcr.20207, 2013.

Costabel, S., Siemon, B., Houben, G. and Günther, T.: Geophysical investigation of a freshwater lens on the island of Langeoog, Germany – Insights from combined HEM, TEM and MRS data, Journal of Applied Geophysics 136, 231–245, 10.1016/j.jappgeo.2016.11.007, 2017.

Costanza-Robinson, M. S., Estabrook, B. D. and Fouhey, D. F.: Representative elementary volume estimation for porosity, moisture saturation, and air-water interfacial areas in unsaturated porous media: Data quality implications, Water Resour. Res., 47, W07513, doi:10.1029/2010WR009655, 2011.

Cundy, A. B., Hopkinson, L. and Whitby, R. L. D.: Use of iron-based technologies in contaminated land and groundwater remediation: A review, Science of The Total Environment 400(1–3), 42-51, 2014.

Cullimore, D. R.: Microbiology of well biofouling, CRC Press, Boca Raton/FL, 456 pp, 2000.

~~Davison, W. and Seed, G.: The Kinetics of the oxidation of ferrous iron in synthetic and natural waters, Geochimica et Cosmochimica Acta 47, 67-79, 1983.~~

Dlugosch, R., Günther, T., Müller-Petke, M. and Yaramanci, U.: Improved prediction of hydraulic conductivity for coarse-grained, unconsolidated material from nuclear magnetic resonance, Geophysics 78 (4), EN55-EN64, 2013.

Dunn, K., Bergman, D. J. and LaTorraca, G. A.: Nuclear Magnetic Resonance - Petrophysical and Logging Applications, Handbook of Geophysical Exploration: Seismic Exploration, Vol. 32 Elsevier Science, Oxford, 312 pp, 2002.

~~Ehrlich, H. L., Ingledew, W. J. and Salerno, J. C.: Iron- and manganese-oxidizing bacteria. In: Shiveley and Barton (1991), 147-170, 1991.~~

Emerson, D., Fleming, E. J. and McBeth, J. M.: Iron-Oxidizing Bacteria: An Environmental and Genomic Perspective, Annual Review of Microbiology 64, 561-583, 2010.

Foley, I., Farooqui, S. A., and Kleinberg, R. L.: Effect of paramagnetic ions on NMR relaxation of fluids at solid surfaces, Journal of Magnetic Resonance Series A 123, 95-104, 1996.

Geroni, J. N. and Sapsford, D. J.: Kinetics of iron (II) oxidation determined in the field; Applied Geochemistry 26, 1452-1457, 2011.

Godefroy, S., Korb, J., Fleury, M., and Bryant, R.: Surface nuclear magnetic relaxation and dynamics of water and oil in macroporous media, Physical Review E 64, 1-13, 2001.

Grunewald, E. and Knight, R.: A laboratory study of NMR relaxation times in unconsolidated heterogeneous sediments, Geophysics 76 (4), G73-G83, 2011.

Haber, F. and Weiss, J.: The catalytic decomposition of hydrogen peroxide by iron salts, Proc. R. Soc. Lond. A 1934 147, 332-351, doi:10.1098/rspa.1934.0221, 1934.

Hazen, A.: Some physical properties of sands and gravels, with special reference to their use in filtration, 24th Annual Rep., Massachusetts State Board of Health, Pub. Doc. No. 34, 539-556, 1892.

Hertzog R.C., White T. A. and Straley C.: Using NMR decay-time measurements to monitor and characterize DNAPL and moisture in subsurface porous media, Journal of Environmental and Engineering Geophysics 12, 293-306, 2007.

Hinedi, Z.R., Chang, A.C. and Anderson, M. A.: Quantification of microporosity by nuclear magnetic resonance relaxation of water imbibed in porous media, Water Resources Research 33 (12), 2697-2704, 1997.

Houben, G. J.: Iron oxide incrustations in wells. Part 1: Genesis, mineralogy and geochemistry, Applied Geochemistry 18 (6), 927-939, 2003a.

Houben, G. J.: Iron oxide incrustations in wells. Part 2: Chemical dissolution and modeling, Applied Geochemistry 18 (6), 941-954, 2003b.

Houben, G. and Weihe, U.: Spatial distribution of incrustations around a water well after 38 years of use, Ground Water 48 (1), 53-58, 2010.

Houben, G. J. and Kaufhold, S.: Multi-Method characterization of the ferrihydrite to goethite transformation, Clay Minerals 46, 387-395, 2011.

Janney, D. E., Cowley, J. M. and Buseck, P. R.: Transmission Electron Microscopy of Synthetic 2- and 6-line Ferrihydrite. Clays and Clay Minerals 48 (1), 111-119, 2000.

Kappler, A. and Straub, K. L.: Geomicrobiological Cycling of Iron, Reviews in Mineralogy & Geochemistry 59, 85-108, 2005.

Keating, K. and Knight, R.: A laboratory study to determine the effects of iron oxides on proton NMR measurements, Geophysics 72 (1), E27-E32, 2007.

Keating, K. and Knight, R.: A laboratory study of the effect of magnetite on NMR relaxation rates, Journal of Applied Geophysics 66, 188-196, 2008.

Keating, K. and Knight, R.: A laboratory study of the effect of Fe(II)-bearing minerals on nuclear magnetic resonance (NMR) relaxation measurements, Geophysics 75 (3), F71-F82, 2010.

Keating, K. and Knight, R.: The effect of spatial variation in surface relaxivity on nuclear magnetic resonance relaxation rates, Geophysics 77 (5), E365-E377, 2012.

Kenyon, W. E.: Petrophysical Principles of Applications of NMR Logging, The Log Analyst 38, 21-43, 1997.

Knight, R., Walsh, D. O., Butler Jr., J. J., Grunewald, E., Liu, G., Parsekian, A. D., Reboulet, E. C., Knobbe, S. and Barrows, M.: NMR logging to estimate hydraulic conductivity in unconsolidated aquifers, Groundwater 54 (1), 104-114, doi: 10.1111/gwat.12324, 2016.

Kolz, J., Goga, N., Casanova, F., Mang, T. and Blümich, B.: Spatial localization with single-sided NMR sensors, Appl. Magn. Reson. 32, 171-184, 2007.

Kozeny, J.: Uber kapillare Leitung des Wassers im Boden: Sitzungsberichte /Akademie der Wissenschaften in Wien, Mathematisch-Naturwissenschaftliche Klasse Abteilung IIa 136, 271-306, 1927.

Larese-and Haderlein, S. B.: Heterogeneous oxidation of Fe(II) on iron oxides in aqueous systems: Identification and controls of Fe(III) product formation, Geochimica et Cosmochimica Acta 91, 171-186, 2012.

Larroque, F. and Franceschi, M.: Impact of chemical clogging on de-watering well productivity: numerical assessment, Environmental Earth Science 64,119-131, 2011.

Legchenko, A., Baltassat, J.-M., Bobachev, A., Martin, C., Henri, R. and Vouillamoz, J.-M.: Magnetic resonance sounding applied to aquifer characterization, Groundwater, 42 (3), 363-373, 2004.

MATLAB®: 9.0.0.341360 (R2016a): The MathWorks Inc., 2016.

~~McBain, J. W.: Oxidation of ferrous solutions by free oxygen, Journal of Physical Chemistry 5(9), 623-638, 1901.~~

Medina, D. A. B., van den Berg, G. A., van Breukelen, B. M., Juhasz-Holterman, M. and Stuyfzand, P. J.: Iron-hydroxide clogging of public supply wells receiving artificial recharge: near-well and in-well hydrological and hydrochemical observations, Hydrogeology Journal 21, 1393-1412, 2013.

Mehra, O. P., Jackson, M.L.: Iron oxide removal from soils and clays by a dithionite-citrate system buffered with sodium bicarbonate, Clays Clay Min. 5, 317-327, 1960.

~~Mohnke, O. and Yaramanci, U.: Pore size distributions and hydraulic conductivities of rocks derived from Magnetic Resonance Sounding relaxation data using multi exponential decay time inversion, Journal of Applied Geophysics, 66, 73-81, doi: 10.1016/j.jappgeo.2008.05.002, 2008.~~

Mohnke, O., Jorand, R., Nordlund, C. and Klitzsch, N.: Understanding NMR relaxometry of partially water-saturated rocks, Hydrol. Earth Syst. Sci. 19, 2763-2773, doi:10.5194/hess-19-2763-2015, 2015.

Müller-Petke, M., Dlugosch, R., Lehmann-Horn, J. and Ronczka, M.: Nuclear magnetic resonance average pore-size estimations outside the fast-diffusion regime. Geophysics, 80 (3), D195-D206, 2015.

Pape, H., Tillich, J. E. and Holz, M.: Pore geometry of sandstone derived from pulsed field gradient NMR, Journal of Applied Geophyiscs 58, 232-252, 2006.

Perlo, J., Danieli, E., Perlo, J., Blümich, B. and Casanova, F.: Optimized slim-line logging NMR tool to measure soil moisture in situ, Journal of Magnetic Resonance 233, 74-79, 2013.

Pham, A. N. & Waite, T. D.: Oxygenation of Fe(II) in natural waters revisited: Kinetic modeling approaches, rate constant estimation and the importance of various reaction pathways, Geochimica et Cosmochimica Acta 72, 3616-3630, 2008.

Prammer, M. G., Drack, E. D., Bouton, J. C. and Gardner, J. S.: Measurements of clay-bound water and total porosity by magnetic resonance logging, Society of Petroleum Engineers, SPE paper 36522, 311-320, doi:10.2118/36522-MS, 1996.

Sapoval, B., Russ, S., Petit, D. and Korb, J. P.: Fractal geometry impact on nuclear relaxation in irregular pores, Magnetic Resonance Imaging 14(7/8), 863-867, 1996.

Schwertmann, U. and Cornell, R. M.: Iron Oxides in the Laboratory – Preparation and Characterization, Wiley-VCH, Weinheim, 188 pp, 2000.

~~Shiveley, J. M. and Barton, L.: Variations in Autotrophic Life, Academic Press, Michigan, 346 pp, 1991.~~

~~Stanjek, H and Weidler, P. G.: The effect of dry heating on the chemistry, surface area, and oxalate solubility of synthetic 2-line and 6-line ferrihydrites., Clay Minerals 27, 397-412, 1992.~~

Stumm, W. and Lee, G. F.: The chemistry of aqueous iron. – Schweizerische Zeitschrift für Hydrologie 22(1), 295-319, 1960.

~~Stumm, W. and Lee, G. F.: Oxygenation of ferrous iron, Industrial and Engineering Chemistry 53(2), 143-146, 1961.~~Stumm, W. and Sulzberger, B.: Cycling of iron in natural environments: Considerations based on laboratory studies of heterogeneous redox processes, Geochimica et Cosmochimica Acta 56, 3233-3257, 1991.

Sucre, O., Pohlmeier, A., Miniere, A., and Blümich, B.: Low-field NMR logging sensor for measuring hydraulic parameters of model soils, Journal of Hydrology 406, 30-38, doi:10.1016/j.jhydrol.2011.05.045, 2011.

Tuhela, L., Carlson, L. and Tuovinen, O. H.: Biogeochemical transformations of Fe and Mn in oxic groundwater and well water environments, Journal of Environmental Science and Health Part A: Environmental Science and Engineering & Toxic and Hazardous Substance Control 32, 407-426, 1997.

Van Dam, R. L., Schlager, W., Dekkers, M. J. and Huisman, J. A.: Iron oxides as a cause of GPR reflections, Geophysics 67(2), P536-545, 2002.

~~Weber, K. A., Achenbach, L. A. and Coates, J. D.: Microorganisms pumping iron: anaerobic microbial iron oxidation and reduction, Nature Reviews Microbiology 4, 752-764, 2006.~~

Weidner, C., Henkel, S., Lorke, S., Rüde, T. R., Schüttrumpf, H. and Klauder, W.: Experimental modelling of chemical clogging processes in dewatering wells, Mine Water Environ 31, 242-251, 2012.

Weidner, C.: Experimental Modelling and Prevention of Chemical Fe-Clogging in Deep Vertical Wells for Open-Pit Dewatering, PhD-Thesis RWTH Aachen University ~~[in German]~~, 219 pp, 2016.

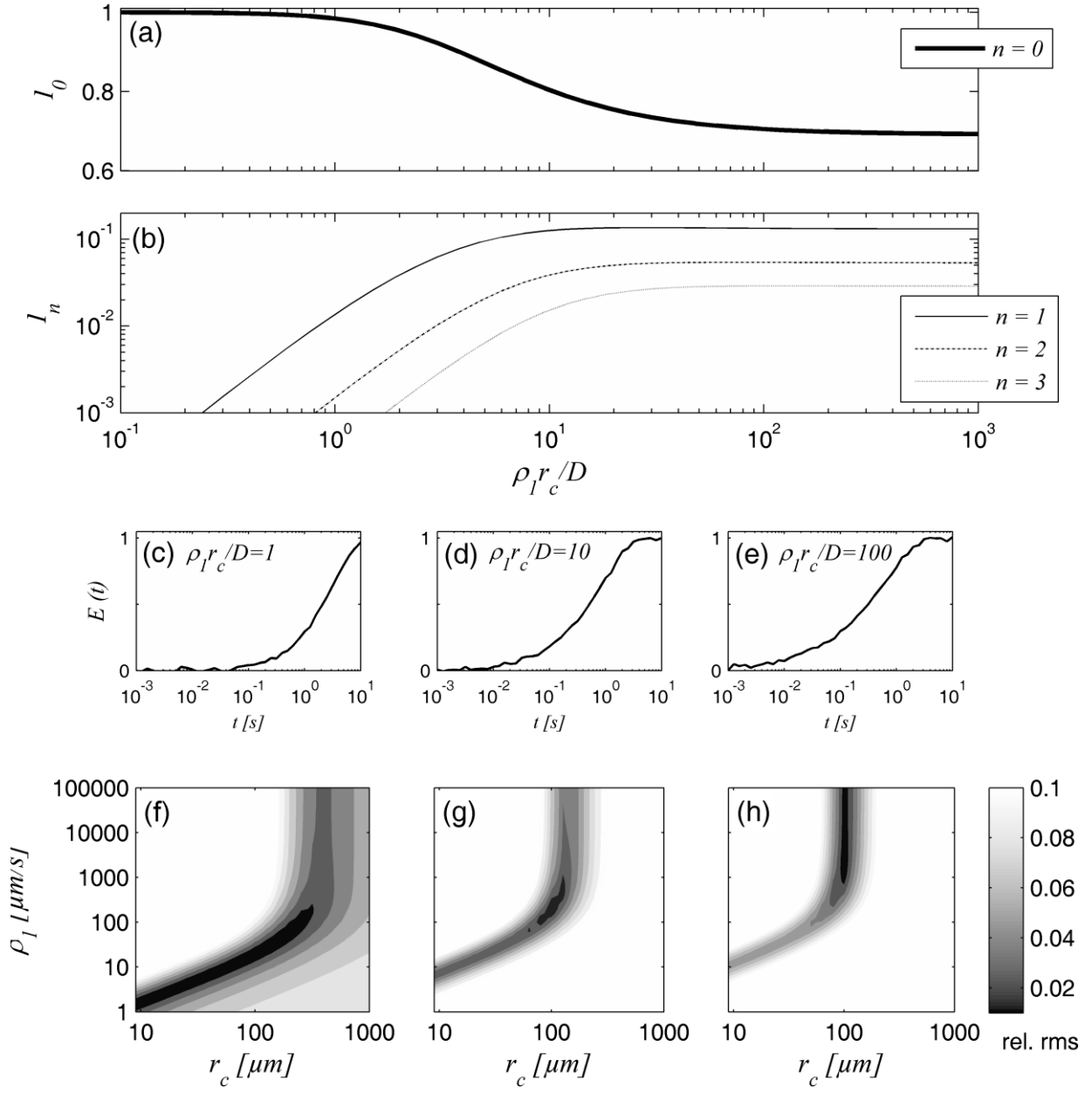

5

Figure 1: (a, b) Intensities of the zeroth to third relaxation modes as functions of the relationship $\rho_1 r_c/D$ visualizing the different diffusion regimes in which NMR relaxation can take place, (c) to (e) simulated T_1 relaxation data for a capillary with (c) r_c = 100

µm and ρ_1 = 20 µm/s, (d) r_c = 100 µm and ρ_1 = 200 µm/s, and (e) r_c = 100 µm and ρ_1 = 2000 µm/s, (f) to (h) corresponding results of a parameter search regarding r_c and ρ_1. The NMR time series was contaminated by Gaussian distributed random noise with an amplitude of 0.01.

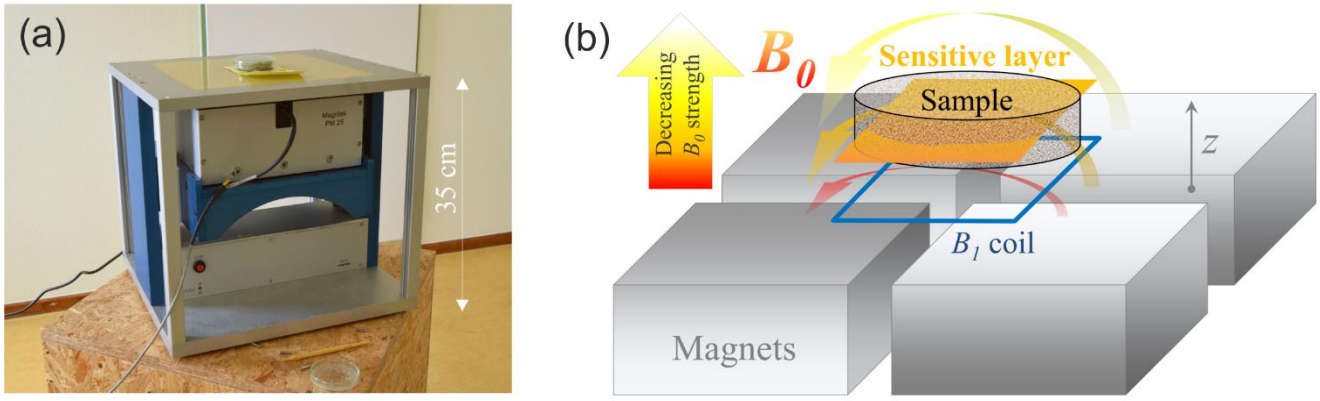

Figure 2: (a) Measurement device and (b) schematic showing the configuration of the permanent B_0-magnets, B_1 coil and the resulting sensitive layer.

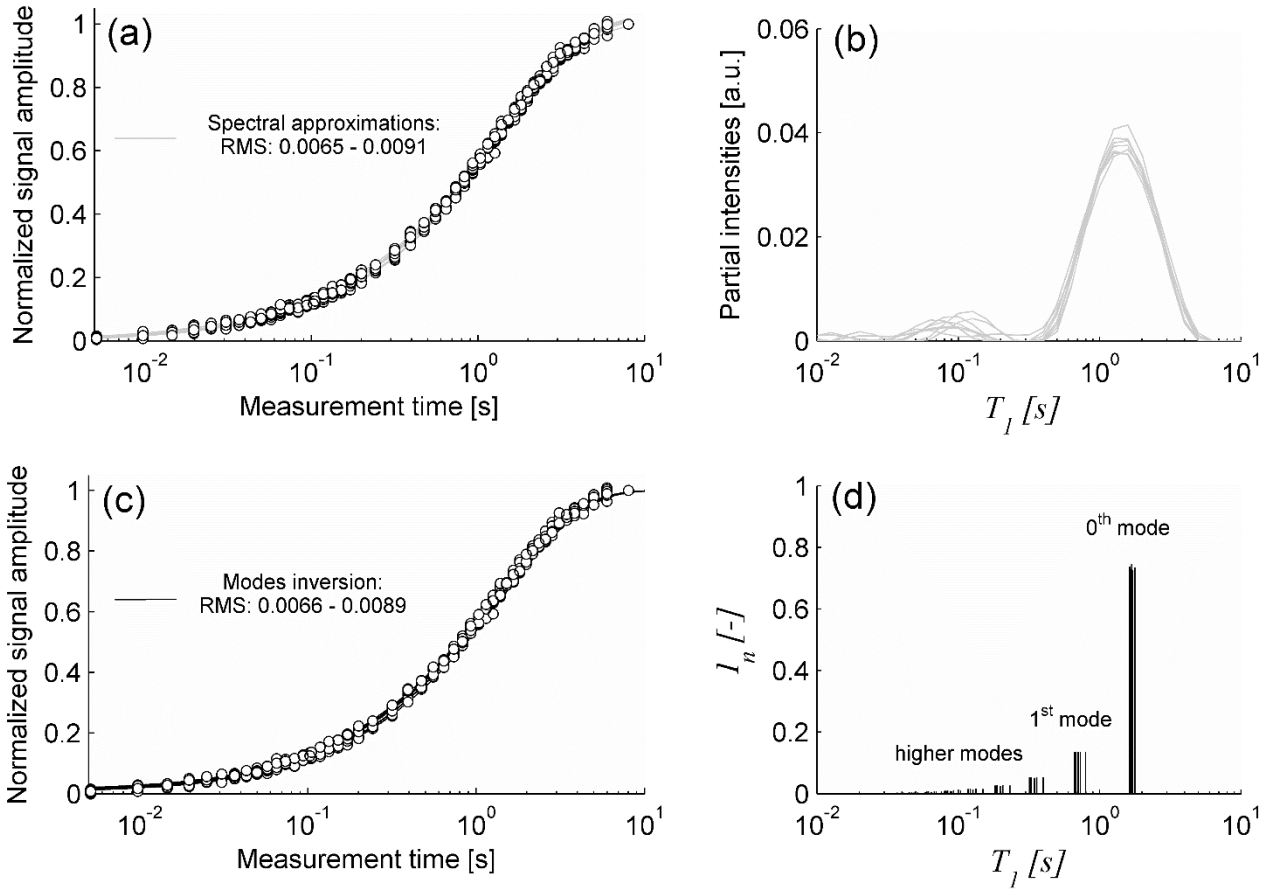

Figure 3: (a) and (c) normalised T_1 measurements at different depth of sample F4 after homogenisation and corresponding approximations using (b) multi-exponential spectrum and (d) relaxation modes.

5

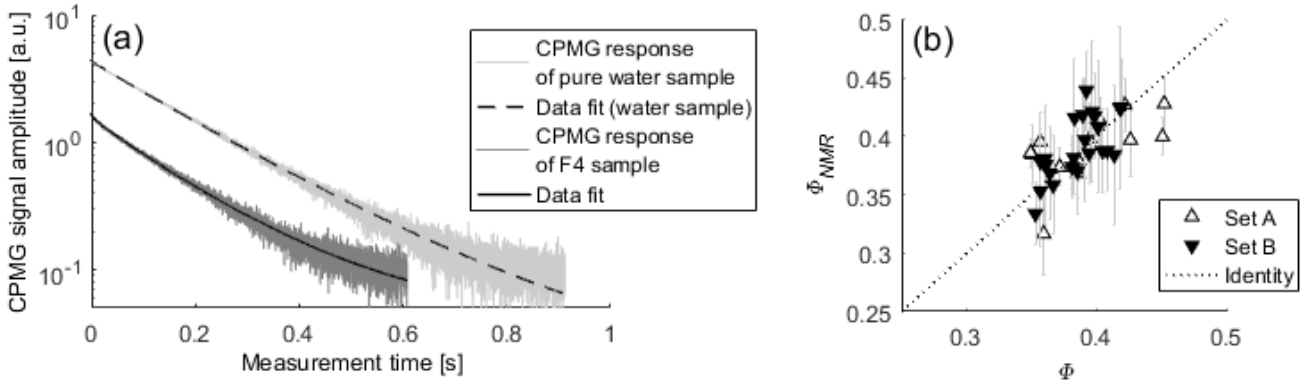

Figure 4: (a) T_2 measurement of sample F4 compared to pure water, (b) NMR-based porosity measurements compared to gravimetrical porosity for all samples.

5

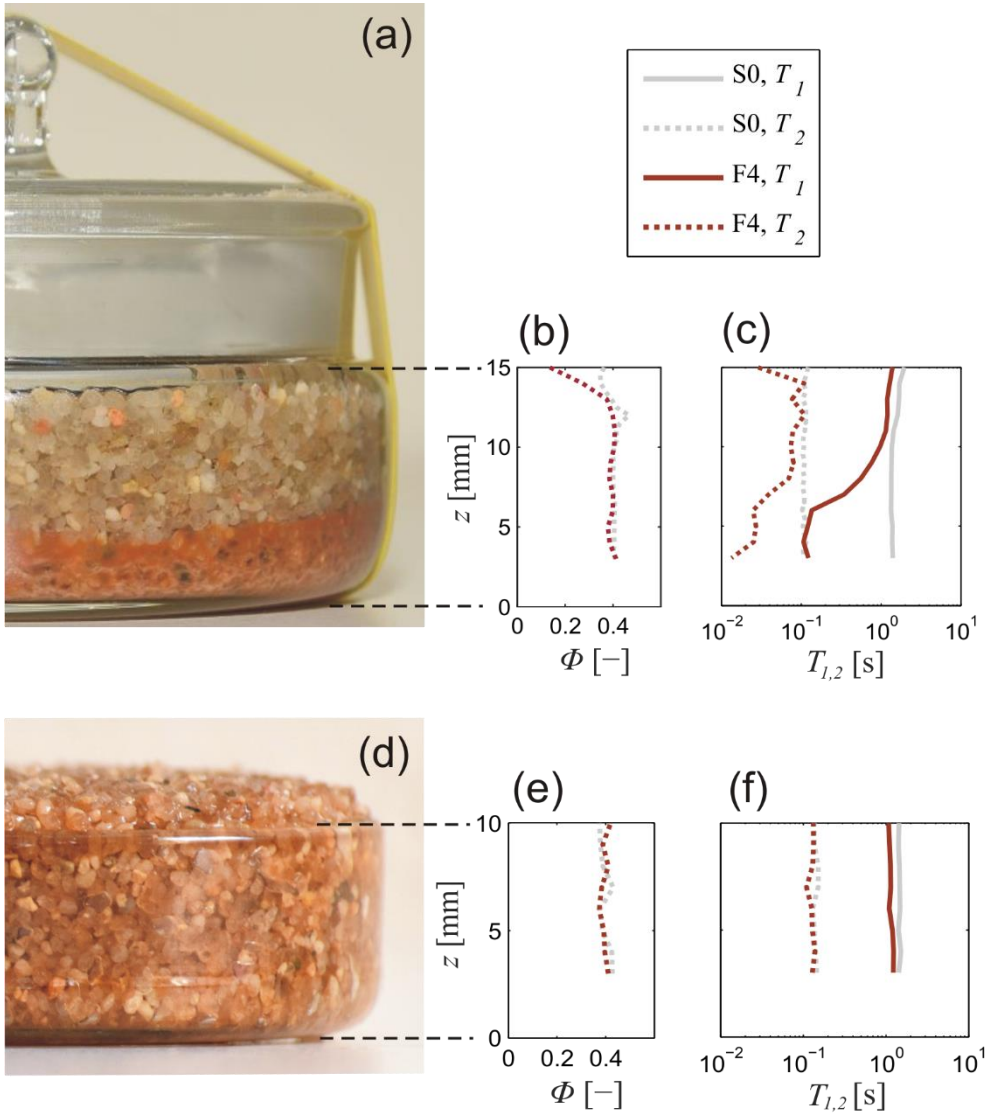

Figure 5: (a) Sample F4 after chemical treatment and precipitation of ferrihydrite particles at the bottom of the sample holder, (b) and (c) vertical distributions of corresponding porosities Φ and mean relaxation times T_1 and T_2, compared to the measurement of untreated sand S0, (d) to (f) sample F4 after homogenisation and corresponding distributions of Φ and $T_{1,2}$.

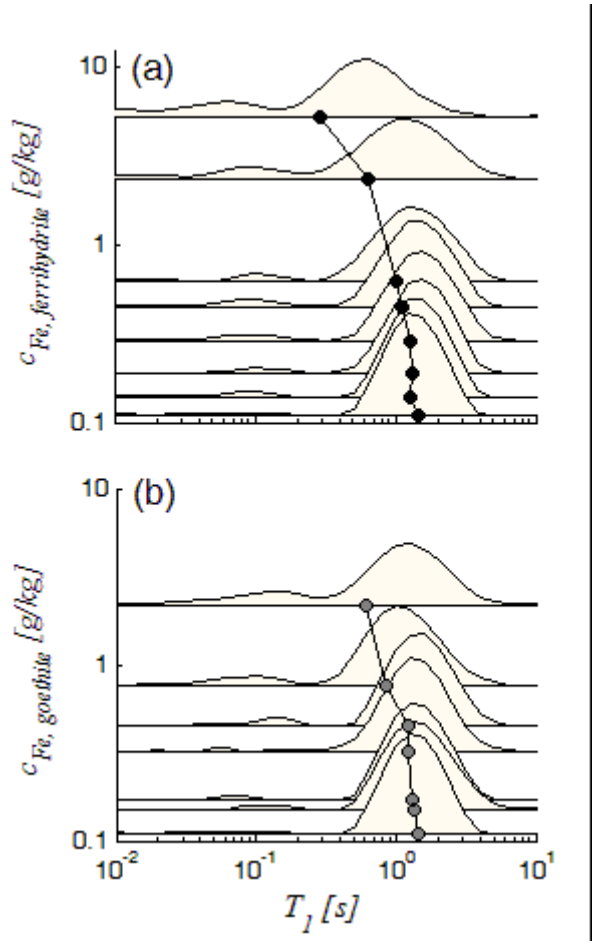

Figure 6: Relaxation time spectra as functions of Fe content for (a) ferrihydrite and (b) goethite samples (Set A), the circles mark the logarithmic mean for each spectrum.

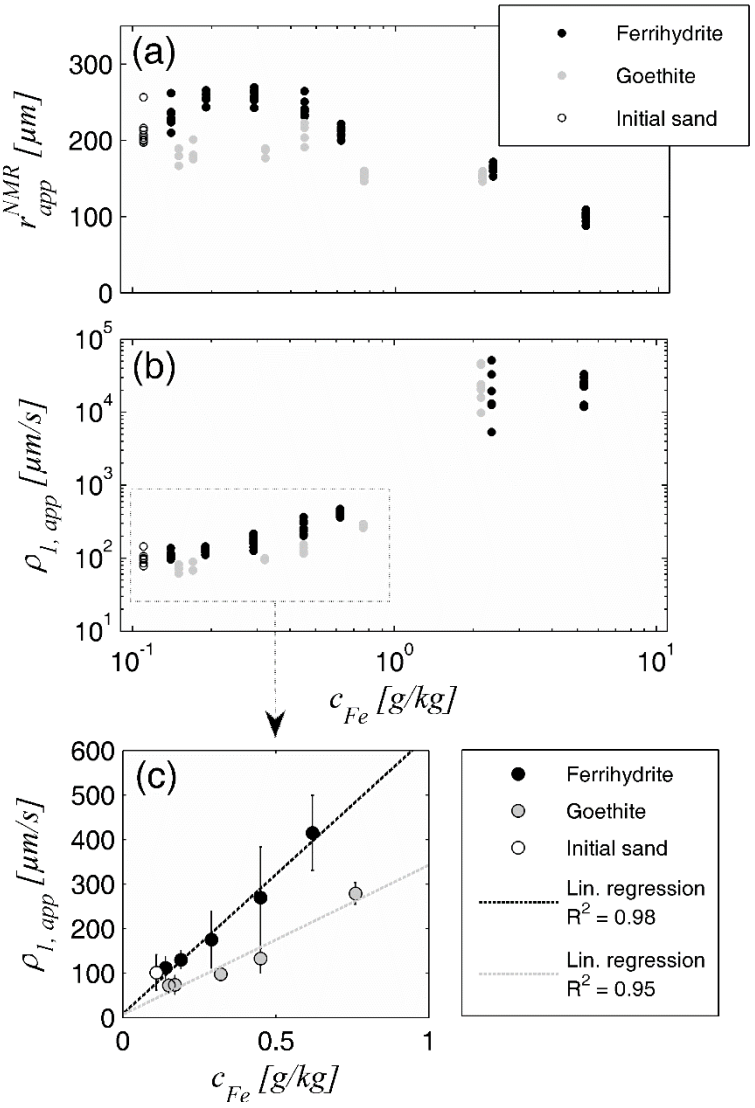

Figure 7: Results of relaxation modes inversion for the ferrihydrite and goethite data sets (Set A): (a) apparent pore radius r_{app}^{NMR} and (b) apparent surface relaxivity $\rho_{1,app}$ as functions of iron content, (c) the mean values and 95% confidence intervals as error bars for Fe contents smaller than 1 g/kg and corresponding linear regression lines, regression coefficient for the ferrihydrite series: 646 µm/s ppm^{-1} (offset: 8.7 µm/s) and for goethite series: 349 µm/s ppm^{-1} (offset: 9.5 µm/s).

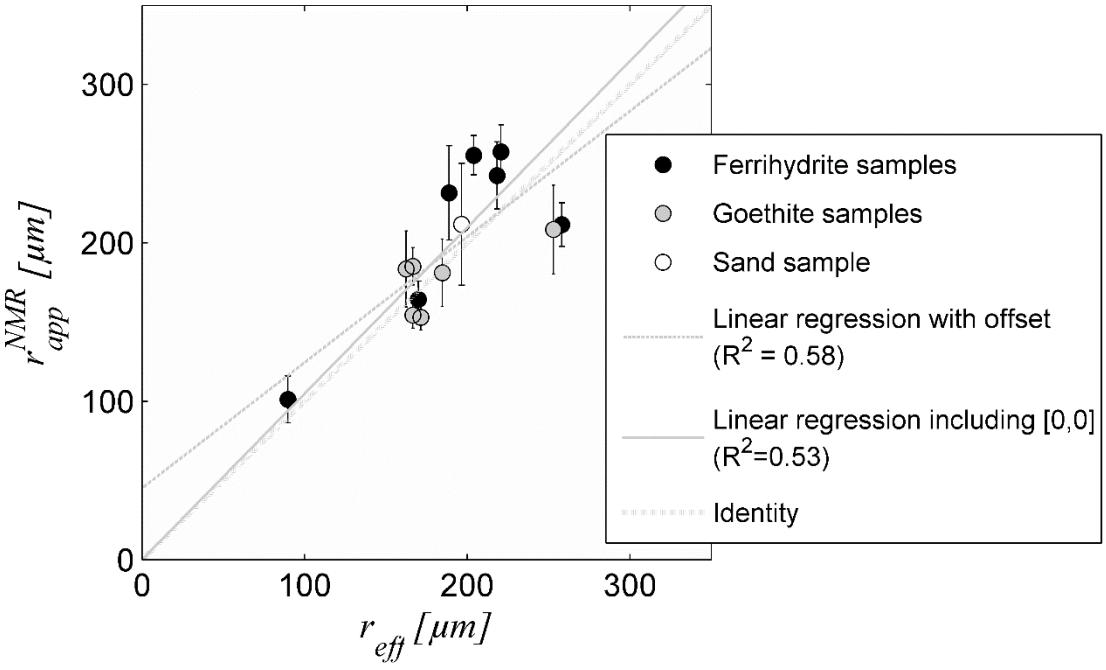

Figure 8: Correlation of effective radius estimates from grain size distribution r_{eff} and the apparent radius estimates from NMR r_{app}^{NMR}, regression coefficient for fitting with constant offset: 0.79, and for fitting without offset, i.e. including the point [0,0]: 1.02.

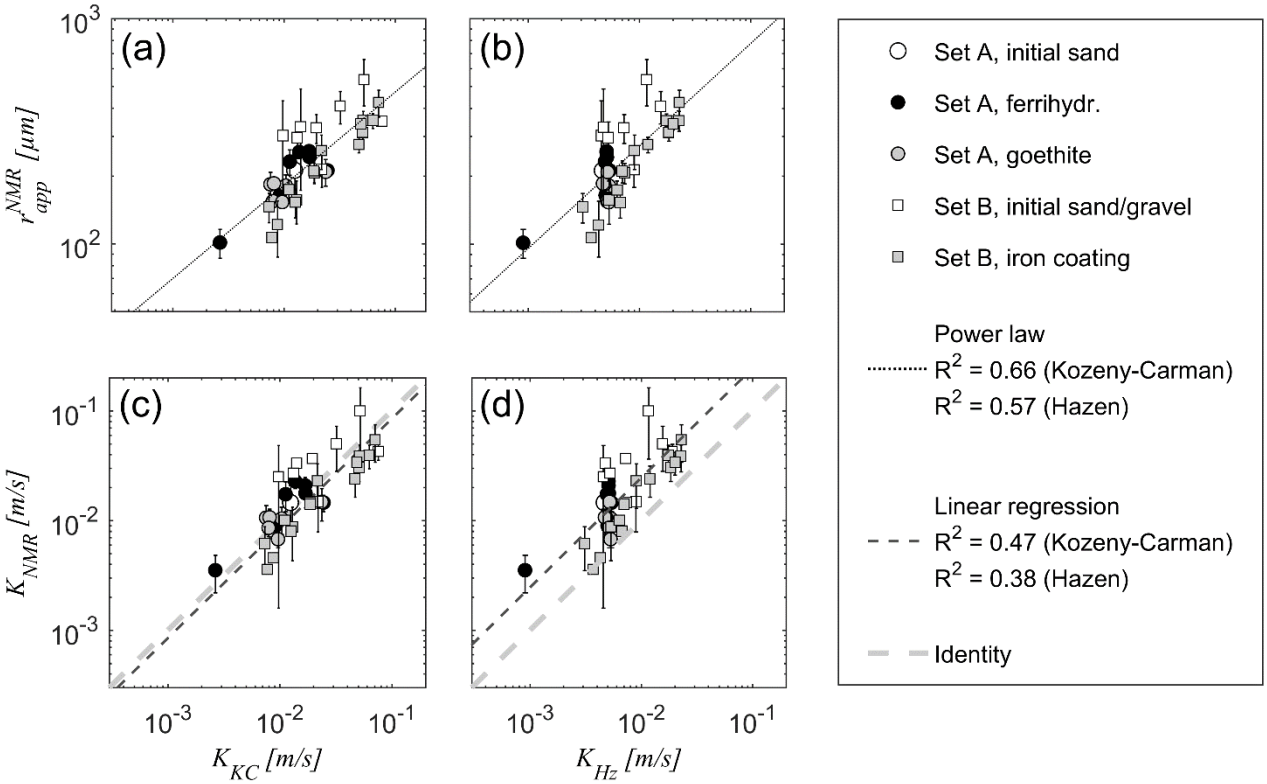

Figure 9: Correlation of NMR-based estimates of apparent radius r_{app}^{NMR} (top) and hydraulic conductivity K_{NMR} (bottom) with reference values for hydraulic conductivity, which are estimated from grain size distribution according to (a, c) Kozeny (1927) and Carman (1939) and (b, d) to Hazen (1892).

Table 1: List of samples with synthetic ferrihydrite (F) and goethite (G) coating (Set A).

Sample	Desired Fe-content [g/kg]	Total Fe-content (XRF) [g/kg]	Dithionite-soluble Fe-content [g/kg]	ϕ (NMR-samples) [m^3/m^3]	d_{60}/d_{10} [µm/µm]	d_{GSD} [µm]	r_{eff} [µm]
F1	10.00	5.88	5.29	0.36	3.27	508	95
F2	5.00	2.94	2.35	0.38	1.43	838	172
F3	2.00	1.26	0.62	0.45	1.40	944	258
F4	1.00	1.05	0.45	0.43	1.42	892	221
F5	0.50	0.91	0.29	0.42	1.41	909	221
F6	0.20	0.77	0.19	0.40	1.42	906	204
F7	0.10	0.63	0.14	0.39	1.43	901	189
G2	5.00	2.73	2.14	0.39	1.44	835	175
G3	2.00	1.40	0.76	0.35	1.42	927	167
G4	1.00	0.98	0.45	0.45	1.41	920	253
G5	0.50	0.91	0.32	0.36	1.45	902	167
G6	0.20	0.70	0.17	0.35	1.44	909	162
G7	0.10	0.77	0.15	0.37	1.39	936	185
S0 [(1)]	0.00	0.84	0.11	0.39	1.47	904	196

[(1)] S0 refers to the original uncoated filter sand.

Table 2: List of samples with artificial and natural iron clogging (Set B).

Sample	Total Fe-content (XRF) [g/kg]	Dithionite-soluble Fe-content [g/kg]	ϕ (NMR-samples) [m^3/m^3]	d_{60}/d_{10} [µm/µm]	d_{GSD} [µm]	r_{eff} [µm]
HB-Z_0 (1)	0.42	0.13	0.39	1.36	1222	261
HB-Z_1 (2)	7.20	7.12	0.39	1.44	935	201
HB41_0 (2)(4)	0.28	0.10	0.39	1.43	1164	247
HB41_1 (2)	2.52	2.39	0.41	1.44	1028	236
HB41_2 (2)	7.90	7.85	0.40	1.48	900	197
HB41_3 (2)	5.74	5.64	0.40	1.46	823	184
GW3151_0 (2)(4)	0.28	0.12	0.38	1.69	1037	213
GW3151_1 (2)	3.64	3.28	0.38	1.46	1180	244
GW5051_0 (1)	1.26	1.08	0.35	1.68	1010	184
GW5051_1 (2)	4.06	3.88	0.36	1.70	856	158
GW3120_0 (2)(4)	0.49	0.25	0.36	1.74	1123	211
GW3120_1 (2)	8.18	8.04	0.36	1.85	917	172
GW3120_2 (2)	14.76	14.80	0.39	1.70	717	155
DF0 (3)	7.48	5.27	0.36	1.51	1719	328
DF11 (3)	10.77	8.26	0.36	1.29	2271	420
DF13A (3)	10.77	8.12	0.39	1.29	2269	474
DF13B (3)	11.33	9.05	0.37	1.36	2092	404
FD0 (3)	5.87	4.45	0.42	1.36	1954	470
FD12A (3)	10.00	8.51	0.40	1.43	1925	436
FD12B (3)	9.02	7.52	0.38	1.39	1958	404
WS0 (3) (4)	0.42	0.17	0.42	1.58	1634	391
WS4 (3)	8.74	8.40	0.40	1.69	1169	258
WS8 (3)	4.69	4.39	0.41	1.57	1586	373

(1) Samples of filter sand and gravel without iron coating taken at dewatering wells excavated in German lignite open-pits (HB: Hambach, GW: Garzweiler);

(2) Samples of filter sand and gravel with natural iron coating taken at dewatering wells excavated in German lignite open-pits;

(3) Samples of filter sand and gravel with artificial iron-coating generated in well clogging experiments (Weidner, 2016) with original material DF0 and FD0 as used in dewatering wells in German lignite mining from three different gravel pits (DF: Dorsfeld, FD: Frimmersdorf, WS: Weilerswist).

(4) Before analysis these samples were treated with dithionite to remove existing surface iron oxides in order to recreate the original state.

Table 3: Estimates of κ according to Eq. ~~14~~ 12 for the samples with artificial ferrihydrite and goethite coatings (Set A).

Sample	κ
F1	11.6
F2	16.3
F3	19.0
F4	10.8
F5	8.6
F6	7.0
F7	6.5
G2	16.4
G3	10.0
G4	11.6
G5	5.2
G6	4.5
G7	5.0
S0	5.4